HHS Public Access

Author manuscript

Cell Rep. Author manuscript; available in PMC 2020 February 26.

Published in final edited form as:

Cell Rep. 2020 January 28; 30(4): 1039–1051.e5. doi:10.1016/j.celrep.2019.12.081.

Treg-Cell-Derived IL-35-Coated Extracellular Vesicles Promote Infectious Tolerance

Jeremy A. Sullivan[1,8,11,*], **Yusuke Tomita**[1,8,9], **Ewa Jankowska-Gan**[1], **Diego A. Lema**[1], **Matt P. Arvedson**[1], **Ashita Nair**[2], **William Bracamonte-Baran**[1,10], **Ying Zhou**[1], **Kristy K. Meyer**[3,4], **Weixiong Zhong**[3,4], **Deepali V. Sawant**[5], **Andrea L. Szymczak-Workman**[5], **Qianxia Zhang**[5], **Creg J. Workman**[5], **Seungpyo Hong**[2,6], **Dario A.A. Vignali**[5,7], **William J. Burlingham**[1]

[1]Department of Surgery, Division of Transplantation, University of Wisconsin–Madison, Madison, WI, USA

[2]Pharmaceutical Sciences Division, School of Pharmacy, University of Wisconsin–Madison, Madison, WI, USA

[3]Department of Pathology and Laboratory Medicine, School of Medicine and Public Health, University of Wisconsin–Madison, Madison, WI, USA

[4]Pathology and Laboratory Services, William S. Middleton Memorial Veterans Hospital, Madison, WI, USA

[5]Department of Immunology, University of Pittsburgh School of Medicine, Pittsburgh, PA, USA

[6]Yonsei Frontier Lab and Department of Pharmacy, Yonsei University, Seoul, Korea

[7]Tumor Microenvironment Center, UPMC Hillman Cancer Center, Pittsburgh, PA, USA

[8]These authors contributed equally

[9]Present address: Department of Surgery, Tokai University, Kanagawa, Japan

[10]Present address: The Johns Hopkins School of Medicine, Baltimore, MD, USA

[11]Lead Contact

SUMMARY

Interleukin-35 (IL-35) is an immunosuppressive cytokine composed of Epstein-Barr-virus-induced protein 3 (Ebi3) and IL-12α chain (p35) subunits, yet the forms that IL-35 assume and its role in peripheral tolerance remain elusive. We induce CBA-specific, IL-35-producing T regulatory (Treg) cells in Treg^{Ebi3WT} C57BL/6 reporter mice and identify IL-35 producers by expression of

*Correspondence: sullivan@surgery.wisc.edu.

AUTHOR CONTRIBUTIONS

Conceptualization, J.A.S., D.A.A.V., W.J.B., and E.J.-G.; Methodology, J.A.S., Y.T., D.A.L., E.J.-G., W.B.-B., W.Z., D.W.S., A.L.S.-W., Q.Z., K.K.M., C.J.W., and S.H.; Investigation, J.A.S., W.J.B., E.J.-G., A.N., D.A.L., M.P.A., and Y.T.; Writing – Original Draft, J.A.S., W.J.B., E.J.G., Y.T., and D.A.A.V.; Writing – Review & Editing, J.A.S., E.J.G., D.A.A.V., C.J.W., M.P.A., and W.J.B.; Funding Acquisition, W.J.B. and D.A.A.V.; Resources, D.A.A.V., W.J.B., and S.H.; Supervision, J.A.S., D.A.A.V., S.H., and W.J.B.

SUPPLEMENTAL INFORMATION

Supplemental Information can be found online at https://doi.org/10.1016/j.celrep.2019.12.081.

DECLARATION OF INTERESTS

The authors declare no competing interests.

Ebi3^{TdTom} gene reporter plus Ebi3 and p35 proteins. Curiously, both subunits of IL-35 are displayed on the surface of tolerogen-specific Foxp3^{+} and Foxp3^{neg} (iTr35) T cells. Furthermore, IL-35 producers, although rare, secrete Ebi3 and p35 on extracellular vesicles (EVs) targeting a 25- to 100-fold higher number of T and B lymphocytes, causing them to acquire surface IL-35. This surface IL-35 is absent when EV production is inhibited or if Ebi3 is genetically deleted in Treg cells. The unique ability of EVs to coat bystander lymphocytes with IL-35, promoting exhaustion in, and secondary suppression by, non-Treg cells identifies a novel mechanism of infectious tolerance.

Graphical Abstract

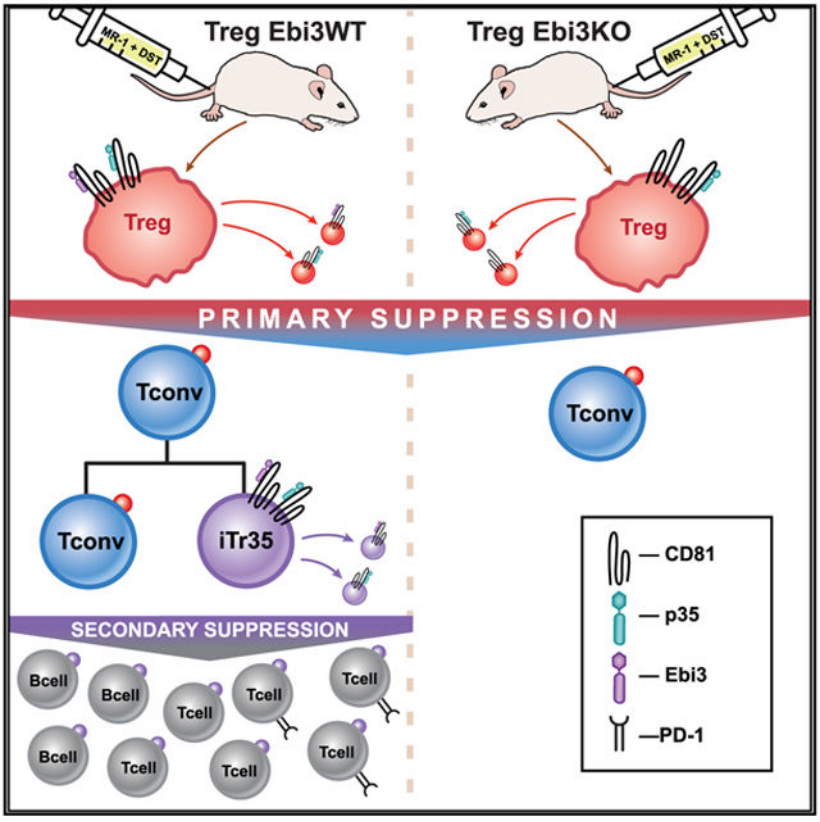

In Brief

Sullivan et al. show that while many factors and cytokines contribute to primary immunosuppression, EV-associated IL-35 uniquely promotes “infectious” tolerance not only by inducing IL-35 production in non-Treg cells but also by causing an immunosuppressive phenotype in EV-acquiring T and B cells, leading to secondary suppression of immune responses.

INTRODUCTION

Antigen-specific T regulatory (Treg) cells have various functions, including reinforcing tolerance to self-antigens encountered in the thymus (tTreg cells) and maintaining tolerance induced to tissue antigens and microbial products encountered peripherally (pTreg cells)

(Abbas et al., 2013). Allo-specific Treg cells may prevent acute rejection and prolong primary graft function after organ transplantation (Takasato et al., 2014; Todo et al., 2016; Geissler, 2012), while eliminating tumor-specific pTreg cells may promote immune rejection of antigenic tumor cells in cancer patients (Turnis et al., 2016; Olson et al., 2012).

Besides lymphoid organs, “memory” Treg cells have been shown to reside in peripheral tissues, including skin (Sanchez Rodriguez et al., 2014). Such cells are capable of imprinting regulatory memory in the tissue, dampening inflammation when the tissue is reexposed to the same antigen (Rosenblum et al., 2011). When a previously tolerated allograft is re-transplanted into a naive allograft recipient, tissue-resident Treg cells are able to overcome the primary acute rejection response of the new host, resulting in graft acceptance (Graca et al., 2002; Li et al., 2012). The tolerogenic impact of such graft-resident Treg cells becomes evident in the setting of severe lymphodepletion of the transplant recipient (Graca et al., 2002; Jankowska-Gan et al., 2012). Even so, their impact is remarkable considering the small number of T cells residing in a skin or kidney allograft and the relatively small percentage of Treg cells within this population.

A standard approach for inducing peripheral allograft tolerance in mice is the transfusion of splenocytes from one strain into another, followed by treatment with anti-CD154 monoclonal antibody (mAb) (MR-1). Indefinite allograft survival across major histocompatibility complex (MHC) and minor H mismatches is induced in the first week, yet the full maturation of the alloantigen-specific Treg cell response appears to require an active process lasting 4–5 weeks (Tomita et al., 2016). This process occurs in distinct phases. Very early changes (within minutes) in the matrix of peripheral lymph nodes guide the trafficking of allo-reactive, Foxp3-negative, conventional CD4 T (Tconv) cells away from sites of productive activation toward areas that favor the preferential expansion of pTreg cells (Warren et al., 2014). However, by day 7, newly arising alloantigen-specific T cells are directed toward anergy rather than a Treg cell fate (Burrell and Bromberg, 2012). By day 14, a mixture of self-specific and allo-specific regulation in spleen and lymph nodes can be detected, and by day 35, the self-reactive component of Treg cell suppression has disappeared, and a purely allo-specific regulation pattern emerges that is stable until at least day 70 (Tomita et al., 2016). Alloantigen-specific T cells were shown by tetramer staining on day 30 to be enriched in Treg cells (Young et al., 2018), and the latter were found to be distributed in both lymphoid and non-lymphoid (e.g., liver) tissue compartments (Tomita et al., 2016). Due to our interest in the disproportionate effects of the small number of Treg cells in non-lymphoid tissues (kidney, liver, lungs, and heart) routinely used in organ transplantation, we wished to determine how relatively few Treg cells at these sites could have such a powerful immunosuppressive impact (Jankowska-Gan et al., 2012; Sullivan et al., 2014, 2017; Olson et al., 2013).

We decided to focus on interleukin-35 (IL-35), a potent immunosuppressive cytokine of the IL-12 family, for several reasons. A heterodimer formed by the glycoproteins Epstein-Barr-virus-induced gene 3 (Ebi3) and the IL-12α chain (p35), IL-35 is produced by $Foxp3^+$ Treg cells and causes primary immunosuppression of T effector responses (Collison et al., 2007). IL-35 appears to play a critical role in infectious tolerance not only by suppressing the proliferation of effector T cells but also by inducing production of IL-35 by non-Foxp3

Tconv cells, known as iTr35 cells (Collison et al., 2010). Other novel IL-35 sources include $CD8^+$ regulatory T cells (Olson et al., 2012), tissue macrophages (Terayama et al., 2014), regulatory B cells (Tedder and Leonard, 2014; Shen et al., 2014; Wang et al., 2014), and dendritic cells (DCs) (Dixon et al., 2015). IL-35 has also been associated with suppression of various autoimmune diseases (Collison et al., 2010; Bettini et al., 2012; Shen et al., 2014) and atherosclerosis (Niedbala et al., 2007; Park et al., 2015).

In addition to its primary immunosuppressive effects, IL-35 was shown to play a key role in T cell exhaustion, as indicated by IL-35-dependent PD1, TIM3, and LAG3 induction on tumor-infiltrating $CD4^+$ and $CD8^+$ T cells, within the tumor microenvironment (Turnis et al., 2016; Sawant et al., 2019). This finding suggests targeting IL-35 might be an alternative to standard checkpoint (anti-PD-1/PD-L1 and CTLA-4/CD86) immunotherapy in the treatment of cancer. Although the precise mechanism is still unclear, anti-Ebi3 antibodies and Treg-cell-restricted deletion of IL-35 expression have been shown to partially rescue anti-tumor immunity in model systems (Collison et al., 2010; Turnis et al., 2016; Olson et al., 2012; Wang et al., 2013; Terayama et al., 2014; Sawant et al., 2019). Yet, for all its known immunoregulatory activities, the instability of the Ebi3/p35 IL-35 heterodimer relative to that of other IL-12 family members has led some to question its importance in Treg-cell-mediated peripheral tolerance (Aparicio-Siegmund et al., 2014).

Perhaps the instability of IL-35 underestimates its true *in vivo* role. For example, the conundrum of rare donor “passenger” DCs nonetheless generating a massive host acute rejection response has recently been traced to their ability to secrete extracellular vesicles (EVs) that “cross-dress” host DCs with alloantigens, greatly amplifying the number of host T cells activated (Marino et al., 2016; Liu et al., 2016). Given the ability of certain types of DC EVs to amplify tolerogenic antigen presentation by inducing PD-L1 expression (Bracamonte-Baran et al., 2017), we hypothesized that IL-35 might be an unusual cytokine that uses an EV rather than a conventional form of cytokine delivery.

To determine how the IL-35 heterodimer behaves in Treg cells and their targets during acquired immune tolerance, we used a standard donor-specific transfusion (DST) + anti-CD154 protocol for induction of peripheral tolerance in B6 mice fluorescently marked for Ebi3 and Foxp3 gene expression. Our studies reveal a previously unknown amplification mechanism whereby relatively few antigen-specific IL-35-producing Treg cells propagate “infectious” peripheral tolerance (Qin et al., 1993) by an EV-based modification of non-Treg cells.

RESULTS

Antigen-Specific Treg Cells and iTr35 Cells Display the Ebi3 Subunit of IL-35 on Their Cell Surface

We first wished to see how IL-35 might enable relatively few antigen-specific Treg cells to leverage a much larger host lymphocyte population in order to propagate tolerance. We used a model of DST, with CBA splenocytes + anti-CD154, to induce allo-tolerance in $Treg^{Ebi3WT}$ (*Foxp3*^{CreYFP} *Ebi3*^{TdTom}) C57BL/6 (B6) mice, as described elsewhere (Tomita et al., 2016; Turnis et al., 2016). Inferences from these “marker” mice were confirmed by

analysis of purified lymphocyte sub-populations from CBA-tolerized wild-type (WT) B6 mice (Figure S1). To quantify the two types of Ebi3 "producers" ($Foxp3^+$ versus $Foxp3^{neg}$), we employed standard and imaging flow cytometry (Figures 1, S2A, and S2B). Using the Ebi3-Td^{tom} marker to follow Ebi3 promoter engagement and an anti-Ebi3 mAb to detect protein expression, we were able to assess those cells that could make Ebi3 protein and those that expressed Ebi3 on its cell surface (Figures 1A and 1B). Among the Treg cells, both the Td^{tom} signal for *Ebi3* gene transcription and that of YFP for *Foxp3* expression were detected (Figure 1A), while "iTr35" cells (Collison et al., 2010) were negative for Foxp3 but positive for *Ebi3* gene transcription (Figure 1B). Using this approach, we analyzed the kinetics of surface Ebi3 expression in Treg cells and iTr35 cells (Figures 1A and 1B, middle panels). On day 14 of CBA tolerization, there was no significant increase in Ebi3 producers among Treg (Figure 1A) and iTr35 (Figure 1B) cells in CBA-tolerized B6 mice as compared to baseline (day 0). By day 35, this difference became highly significant ($p < 0.001$), as the frequency of IL-35 producers among both types of $CD4^+$ T cells rose 10-fold. Importantly, Ebi3 production at all time points was abolished by genetic deletion of *Ebi3* in $Foxp3^+$ cells only ($Foxp3^{CreYFP}$ $Ebi3^{loxP/loxP}$; $Treg^{Ebi3KO}$).

To test for a memory Treg cell response, we harvested lymph node cells (LNCs) on day 35 and cultured them overnight with CBA, self-, or third-party DBA/2 antigens (Figures 1A and 1B, bottom panels). By flow cytometry analysis, we found two distinct patterns of endogenous expression: (1) $CD4^+$ Treg cells expressing both surface Ebi3 protein as well as the internal markers for *Foxp3* and *Ebi3* gene transcription and (2) $CD4^+$ iTr35 cells expressing Td^{tom} but lacking Foxp3 expression. Both were increased 2- to 3-fold upon *in vitro* reexposure to CBA antigen. This increase was significant (*$p < 0.01$ versus media control) in both Treg cells and iTr35 cells. An increase over baseline (media) levels was seen with CBA, but not autologous B6 or third-party DBA/2 control antigens, indicating an antigen-specific memory Treg cell response. Targeted deletion of *Ebi3* in $Foxp3^+$ $CD4^+$ T cells of tolerized mice ($Treg^{Ebi3KO}$) eliminated not only the baseline expression of surface Ebi3 on cells at day 35 but also the CBA-induced increase in both Treg and iTr35 cells (Figures 1A and 1B). Imaging flow cytometry analysis of the Td^{tom} and YFP signals confirmed internal localizations of both YFP and Td^{tom} gene reporter signals (Figure S3). Cell-surface expression of Ebi3 protein (Figure S3C) was in keeping with its original description (Devergne et al., 1996) but nonetheless somewhat surprising in the absence of a transmembrane domain or known GPI linkages of either the Ebi3 subunit itself or its known partners, p28 (IL-27) and p35 (IL-35).

Exogenous Surface IL-35 Expression Is Passively Acquired from IL-35 Producers

In contrast to the rarity of endogenous Ebi3 producers (5–20 cells/10^6), a much larger number of $CD4^+$ T cells (200–600 cells/10^6) displayed only exogenous surface expression; i.e., they lacked any internal Ebi3 signal but showed surface expression of Ebi3 protein (sEbi3) both directly *ex vivo* on day 35 and after overnight culture with antigen (Figure 1C, top). In contrast to the slow development of detectable, endogenous expression following tolerization, we found a significant increase over baseline IL-35 exogenous expression among $Td^{tom\text{-}neg}$ $CD4^+$ T cells as early as 14 days post-tolerization, peaking at an average level of 200/10^6 $CD4^+$ T cells on day 35 (Figure 1C, middle). The specificity of exogenous

IL-35 expression paralleled that seen for endogenous expression on day 35, with a 3-fold increase in frequency, from $200/10^6$ up to $600/10^6$ being induced by overnight culture with specific CBA tolerogen. This compares with no increase in exogenous IL-35 over media control following autologous B6 or DBA/2 third-party control antigen stimulation (Figure 1C, bottom).

In the example shown (Figure 1C, top), zones of acquired sEbi3 are shown dotting the surface of a YFP^{neg}, $Td^{tom\text{-}neg}$ Tconv cell. This punctate expression pattern was not limited to Tconv cells and was also seen on YFP^+, $Td^{tom\text{-}neg}$ $CD4^+$, non-Ebi3-producing Treg cells (Figure S2). Such a phenotype would suggest either (1) a formerly endogenous producer that has ceased to produce IL-35 while remaining IL-35^+ at the protein level or (2) exogenous expression due to passive uptake of IL-35 from Treg or iTr35 cells actively producing this cytokine.

To exclude the former possibility, we restimulated day 35 CBA-tolerized B6-$Thy1.2^+$ LNC in transwell cultures with CBA (specific tolerogen), B6 (syngeneic), or DBA/2 (third-party) cell-free antigen in the top well. We found a tolerogen-specific increase in surface Ebi3 immunostaining among naive $Thy1.1^+$ B6 LNCs in the bottom well after overnight culture (Figure 1D). Thus, this form of surface cytokine expression could be passively acquired by $CD4^+$ Tconv "bystander" lymphocytes. The effect was antigen specific. When corrected for media "background," there was a significantly greater increase in sEbi3 expression on $Thy1.1^+$ $CD4^+$ T cells in bottom-well cultures when top-well LNC cultures from individual mice were restimulated with allo-specific CBA antigen as compared with B6 or DBA/2 antigen ($p < 0.005$ versus both B6 and DBA/2; Figure 1D, right). To rule out any effects on IL-35 production, further transwell experiments were carried out using CBA-tolerized LNCs restimulated with CBA or DBA/2 antigen in the top well, while LNCs from mice that are null for Ebi3 ($Ebi3^{KO}$) were placed in the bottom well (Figure 1D, far right). We observed a dramatic increase in the number of $Ebi3^{KO}$ but $sEbi3^+$ $CD4^+$ T cells after overnight CBA versus DBA/2 stimulation (Figure 1D, bottom left). This increase in $sEbi3^+$ expression by $CD4^+$ T cells from $Ebi3^{KO}$ mice was abolished by a 4-h pretreatment of CBA-tolerized LNCs in the top well with GW4869, a neutral sphingomyelinase inhibitor (Figure 1D, far right) reported to inhibit EV production (Kosaka et al., 2010; Li et al., 2013). While not ruling out other explanations (for example, although toxicity was minimal at the dose used, other neutral-sphingomyelinase-specific effects of GW4869 are possible), the data suggest that, rather than simply being "burned out" producers, the high frequency of non-producer T cells with sEbi3 expression were likely the recipients of IL-35^+ EVs released by rare Treg cells and iTr35 "endogenous" IL-35 producers.

IL-35 "Cross-Dressed" Lymphocytes Are Lineage Heterogeneous and Express Checkpoint Inhibitors

Having established that ~1% of $CD4^+$ Tconv cells were altered by IL-35 in tolerant mice, we wished to see if this effect was confined only to $CD4^+$ T cells or if other types of lymphocytes were involved. We first tested day 35 LNCs for acquisition of sEbi3 as a marker of surface IL-35 acquisition by various lymphocyte subsets. We identified cross-dressed IL-35^+ cells among "non-producer" $CD4^+$, $CD8^+$ T and B lymphocytes by $sEbi3^+$

phenotype in the absence of internal Td^{Tom} signal. By far the largest frequency of such cells was found among the $CD4^+$ $Foxp3^{neg}$ Tconv and B cells (Figure 2A). These were followed numerically by $CD8^+$ T cells and lastly by $CD4^+$ $Foxp3^+$ Treg cells (Figure 2B). However, the latter were key to this acquired IL-35 phenotype; when Ebi3 knockout (KO) was restricted to $Foxp3^+$ cells ($Treg^{Ebi3KO}$), both T and B cells tested on day 35 post-tolerization failed to show acquired surface IL-35 expression (Figure 1C; data not shown). Examples of exogenous, surface Ebi3 on $CD4^+$ and $CD8^+$ T and B lymphocytes by standard and imaging flow cytometry are shown in Figure 2C. Note the punctate manner of sEbi3 immunostaining by Image-Stream analysis of $CD4^+$ Tconv, $CD8^+$ T, and B cells.

Turnis et al. (Turnis et al., 2016; Sawant et al., 2019) previously reported high levels of the inhibitory receptors (IRs) PD1, LAG-3, and TIM-3 on tumor-infiltrating $CD4^+$ and $CD8^+$ T lymphocytes; this was abolished by Treg-cell-restricted *Ebi3* deletion. Using the same reporter mice, we first quantitated sEbi3 producers among different LNC subsets post-tolerization. We found that $CD4^+$ Treg, $CD4^+$ Tconv, $CD8^+$ T, and B cell subsets all contained rare endogenous Ebi3 producers on day 35; the difference between day 0 and day 35 production was significant in all four subsets tested ($p < 0.01$–0.001; Figure S4). To determine the functional consequences of exogenous IL-35 expression, we examined the 100-fold more frequent, EV-altered cells for expression of IRs in LNC on day 35. Compared with their $sEbi3^{neg}$ counterparts, we found that $sEbi3^+$ LNCs ($CD4^+$, $CD8^+$ T, and non-T lymphocytes) all showed 3- to 10-fold increased levels of PD1, LAG3, and TIM3 expression ($p < 0.01$;Figures 2D-2F). Interestingly, $Treg^{Ebi3KO}$ mice did not show any significant increase in PD1 expression on their $CD4^+CD25^{neg}$ T, $CD8^+$ T, or B lymphocytes on day 35 after tolerization (data not shown). Taken together, these data suggest that the pattern of IR expression seen in tolerized, allograft-reactive T cells, as well as that reported previously on tumor-infiltrating T cells (Turnis et al., 2016; Sawant et al., 2019), is restricted to EV-modified, IL-35 cross-dressed T and B cells.

Co-expression of Ebi3 and p35 on the Surface of IL-35 Producer and Acceptor T Cells

To determine whether Ebi3 alone or both chains of IL-35 were surface expressed on $CD4^+$ Ebi3 producers, we co-stained CBA-restimulated LNCs with anti-Ebi3 and p35 antibodies. As shown in Figure 3A (Treg cell) and Figure 3B (iTr35 cell), both chains of IL-35 were distributed broadly on the surface of producer T cells. The frequency (number of IL-35-positive cells/10^6 $CD4^+$ T cells) of surface Ebi3/p35-double-positive producers increased 2- to 3-fold relative to media control in response to CBA, but not B6 or DBA antigen, rechallenge *in vitro* (Figures 3A and 3B). The bright detail similarity index (BDSI) values for sEbi3 and p35, a measure of co-localization, were consistently >1 but rarely >2, indicating that the two chains were somewhat co-localized on the cell surface. In contrast, BDSI values for p35 and CD4 were consistently <1, indicating comparatively poor co-localization (Figures S5A and S5B).

While Ebi3/p35 double producers were found at a lower frequency than Ebi3 single-producer T cells (compare Figures 1A and 1B with Figures 3A and 3B), exogenous expression of both chains of IL-35 by non-producers was again seen at a much higher (~20–100×) level (Figure 3C). The acquisition of sEbi3/p35 by non-producer T cells (exogenous

expression) in antigen-stimulated cultures on day 35 after tolerization followed the same pattern of allo-antigen specificity seen previously with sEbi3 alone. CBA-specific antigen stimulation increased this frequency 2- to 3-fold relative to media control in response to CBA, while neither B6 nor DBA antigen rechallenge *in vitro* did so (Figure 3C, bottom left). While there was no YFP or Td^{tom} signal, both the sEbi3 and p35 proteins were expressed on the cell surface. Average BDSI values for sEbi3-p35 association, regardless of antigen used for restimulation, were not different between endogenous (Figures 3A and 3B) and exogenous (Figure 3C) expression, both being in the 1.2–1.4 range (Figures S5A and S5B versus Figure S5C). Closer examination of the co-localization of the sEbi3 and p35 signals indicates that surface patches clearly contain signals for both sEbi3 and p35, indicating zones of IL-35 on the surface of the cell (Figure 3C, right; see also Figure S5D). This phenomenon of EV-based surface IL-35 expression was not limited to CBA→ B6 tolerogenesis. Using a completely different tolerization system (B6 × BALB/$c^{mOva\text{-}2W1S}$ F1 spleen cells→B6) as the source of DST along with MR-1 treatment (Young et al., 2018), we could replicate antigen-specific tolerance and identify peptide/MHC-specific surface IL-35^+ Treg cells by tetramer and IL-35 subunit co-staining (Figure S6).

IL-35-Coated EVs Are Produced in Tolerized B6/Alloantigen Co-cultures

To explain both the low frequency of IL-35 producers and the wide dissemination of exogenous IL-35 expression on non-Treg cells, we isolated EVs by ultracentrifugation from culture supernatants after 24-h *in vitro* restimulation of CBA-tolerized (day 35) B6 mouse splenocytes with either DBA (third party), CBA antigen, or media control. As shown in Figure 4A, by standard transmission electron microscopy (TEM), these EVs had a typical round appearance. Using nanoparticle tracking analysis (NTA), the particles released after restimulation predominantly showed a mean particle size range between 50 and 200 nm (Figures 4B and S7). The number of particles released per cell ranged from 250 to 450 (Figures 4C and S7). To further implicate an EV-mediated transmission of IL-35 to bystander cells, the tetraspanin CD81 plus p35 and Ebi3 were detected by western blot in isolated EV of co-culture supernatant, but not in EV/exosome-free fractions remaining in the supernatant after 100,000 × *g* ultracentrifugation (Figure 4D). Antibodies to either Ebi3 or p35 were able to co-precipitate CD81 protein from the EV fraction, indicating association of Ebi3 and p35 with CD81 on/in the EV under non-reducing conditions (Figure 4E).

Using a CD81-specific mAb for detection, with various capture antibodies, we quantitated by ELISA the expression of EV proteins (i.e., those present only in the 100,000 × *g* pellet). For example, $CD81^+$ EVs in this fraction were captured with p35 or Ebi3-specific mAbs, while no signal was detected in the supernatant of the 100,000 × *g* centrifugation (Figure 4F). Note that a p28 (IL-27/IL-30)-specific mAb capture of EVs did not yield a signal above the immunoglobulin G_{2b} (IgG_{2b}) background (Figure 4F). Furthermore, unlike IL-10, which was detected exclusively in the supernatant and not the 100,000 × *g* pellet, ELISA experiments using only Ebi3 detection and p35 capture antibodies showed that IL-35 was not in the supernatant and only in the 100,000 × *g* pellet (Figure S1). Besides IL-35, $CD81^+$ EVs were also captured with CD39- and CD73-specific antibodies (Figure 4G). In contrast to detection with anti-CD81, ELISAs using antibody to a different tetraspanin, CD9, failed to detect Ebi3 or p35 signals (Figure 4H), although other $CD9^+$ EVs, such as those

previously associated with DCs (Bracamonte-Baran et al., 2017), were found in these culture supernatants. Figure 4I shows CD81 expression was enriched in the EV– fraction of culture supernatant, while the Golgi (GM130), endoplasmic reticulum (ER) (gp96), and secretory (calnexin) apparatus proteins were associated with cellular material precipitated at low centrifugal speeds.

Finally, we used TEM-immuno-gold labeling of CD81, p35, and Ebi3 to confirm their co-localization in the EV compartment. As illustrated in Figure 4J, we collected EV by ultracentrifugation of culture supernatant from CBA-tolerized B6 LNCs restimulated with CBA antigen overnight and performed immuno-gold staining. We could detect the presence of gold nanobeads for CD81 (~15 nm) and p35 (~6 nm) (left panels) or CD81 (~15 nm) and Ebi3 (~10 nm) (right panels) on individual EVs. Additionally, we could also visualize co-staining of individual EVs for both IL-35 subunits (Figure S7).

Abolition of IL-35 in Treg Cells Reveals Alternative Mechanisms of Primary Suppression by EV but the Absolute Requirement of IL-35^{+} EVs for Secondary Suppression

To determine antigen specific-inhibitory potential of EVs, we used the *trans vivo* delayed type hypersensitivity assay (tvDTH)-linked suppression assay. Briefly, spleens from B6 tetanus toxoid (TT)-immunized B6 mice were used as the responder cells in the tvDTH assay in the presence or absence of TT, along with EV collected from cultures of day 35 CBA-tolerized Treg^{Ebi3WT} mice restimulated with either CBA (allo-) or DBA (third-party) antigen. While strong inhibition of TT-specific tvDTH was seen with CBA-antigen-induced EV, only slight inhibition was seen with EV from DBA/2 restimulation cultures, indicating antigen-specific induction of suppression (Figure 5A). Interestingly, when we compared the ability of EV from tolerized Treg^{Ebi3WT} mice with those from CBA-tolerized mice with Treg-cell-specific Ebi3 deletion (Treg^{Ebi3KO}) to inhibit a TT-specific tvDTH response, all EVs suppressed equally well; however, only those from the former did so in an IL-35-dependent manner (Figure 5B versus Figure 5C). In Treg^{Ebi3KO} mice, EV-associated, CD39-dependent, ARL67156-sensitive (Figure 5C), and EV-independent transforming growth factor β1 (TGF-β1)- and IL-10-dependent suppression (Figure S8) remained, but IL-35-dependent primary suppression was abolished. To determine the primary functional effects of tolerogenic EV in a transplant model, EVs harvested from day 35 cultures of CBA-tolerized Treg^{Ebi3WT} or Treg^{Ebi3KO} mice restimulated with CBA antigen overnight were injected on day 0 of a CBA→B6 mouse heart transplant. We observed a >3-fold prolonged median heart graft survival, from 7.3 (media control) to >22 days, in both the Treg^{Ebi3WT} and Treg^{Ebi3KO} EV-treated mice compared to only a 2-day prolongation of mean survival time with EVs from DBA/2-antigen restimulated cultures (Figure 5D). Thus, suppressive EV production required antigen-specific stimulation, but IL-35, as just one of multiple EV-based mechanisms causing primary suppression, could be eliminated without altering short-term tvDTH suppression or transplant prolongation.

As previously shown (Figure 2), a unique feature of IL-35 is its ability to cause IRs (LAG3, TIM3, and PD1) to appear on EV-cross-dressed T and B cells, leading to an “exhausted” status (Turnis et al., 2016). Besides such “self-suppression,” another possible outcome of cross-dressing by EV IL-35 might be to equip that cell to suppress another (e.g., bystander

third-party T cells contacted when entering the tissue). To test this idea, we added EVs from overnight cultures of CBA-tolerized Treg^{Ebi3WT} hosts to “naive” B6 LNCs. This caused sEbi3 and p35 expression to appear on ~1.2% of the co-cultured B6 cells (see example in Figure 5E, top). Surface Ebi3 expression was reduced to background levels (~0.3%) using EVs from day 35 CBA-tolerized Treg^{Ebi3KO} mice (data not shown). To determine if surface IL-35 components expressed by these EV cross-dressed cells could still form active IL-35 and give rise to secondary suppression, we mixed T cells that had been incubated with EVs from CBA-tolerized Treg^{Ebi3WT} or Treg^{Ebi3KO} B6 mice with TT-immunized B6 SCs at varying ratios in a standard tvDTH assay (Figure 5E). If the EVs came from tolerized mice that were deficient for IL-35 in their Foxp3$^+$ T cells (Treg^{Ebi3KO}), no significant suppression of TT-specific tvDTH was observed relative to media-treated control B6 T cells. However, B6 T cells that had been pre-incubated with EVs from CBA-tolerized Treg^{Ebi3WT} mice caused significant ($p < 0.02$) suppression compared with Ebi3-KO EV-treated B6 T cells or T cells treated with media alone (Figure 5E; $p < 0.002$). Note that secondary suppression was observed across varying ratios (1:4–1:1) of modifier/TT-sensitized cells. These findings support the concept that IL-35 allo-specific tolerogenesis is indeed mediated and spread by EVs.

DISCUSSION

The unique features of IL-35-based immune regulation are summarized in Figure 6. In the example shown, CD81-associated subunits p35 and Ebi3 are released from a Treg cell (red) after EV formation within a vesicle and its fusion with the plasma membrane (Figure 6, left). Alternatively, in the case of lymphocytes, the EV may form directly at the plasma membrane (Figure 6, left). The released EV contains inhibitory microRNA (miRNA) and features CD39, as well as CD73 (not shown), along with CD81 and associated molecules (e.g., p35 and Ebi3) on its surface. All of these components mediate primary immune suppression, acting on the effector T cell (blue, Figure 6, right). However, unlike other EV components, not all tetraspanin-associated IL-35 is routed to the lysosome for destruction, as a portion is rerouted to the cell surface. There, IL-35 subunits recombine to tonically cause secondary “*cis*” effects (leading to “exhaustion”) as well as a secondary “*trans*” effects, suppression of newly arriving, bystander T effector cells, by interacting with IL-35R on another cell’s surface. The model suggests that production of EV containing the two subunits of IL-35, in association with CD81, is a process initiated by Treg cells. However, EVs containing both IL-35 components were ultimately made by different elements of the immune system, including both iTr35 and B cells as well as iTreg cells (Figures 1,2, 3, S1, and S4). Besides these producers, many more lymphocytes become cross-dressed by IL-35$^+$ EVs, accounting for the much higher frequency of exogenous versus endogenous expression of IL-35 during infectious tolerance.

We found that Treg cells displayed both components of IL-35 in a membrane-associated form, diffusely over the cell surface. IL-35 subunits were not released as a water-soluble heterodimer but rather as components of EVs, previously shown to be the mechanism for delivery of suppressive miRNA (Okoye et al., 2014), and CD39/CD73 ecto-enzymes (Agarwal et al., 2014) from Treg cells to Tconv cells. The IL-35-coated EVs were produced by relatively low numbers of antigen-specific Treg cells, iTr35 cells, and B cells but targeted

a high-frequency population of non-producer $CD4^+$ Tconv and $CD8^+$ T cells, as well as B cells (Figure S4), which then displayed both Ebi3 and p35 subunits on their cell surfaces (Figures 1, 2, and 3). Moreover, IL-35 acquired via EVs expressed on the cell surface was still active, as indicated by the unique ability of IL-35 EV-modified cells to suppress a tvDTH response (Figure 5E). *In vivo*, the induction of multiple IRs (PD-1/LAG3/TIM3) previously associated with IL-35 production by Treg cells (Turnis et al., 2016) was found to be confined to EV-modified cells, thereby "marked" with lymphocyte-derived, IL-35-coated EVs.

Vaidyanathan et al. (2003) noted that when p35 is produced as a component of IL-12, the rate-limiting step for IL-12 secretion was the cleavage of the p35 signal peptide membrane anchor region, releasing the protein into the Golgi cisternae. In the case of IL-35, this type of secretion event does not appear to have occurred. Instead, both p35 and Ebi3 became CD81 associated and were secreted as plasma-membrane-associated, EV-transported molecules by rare "IL-35-producer" lymphocytes. Once packaged and released as EV components during tolerance induction by low-frequency Treg cells and Treg-cell-"deputized" T, iTr35, and B cells, IL-35 was then acquired by log-fold greater numbers of non-producing, bystander lymphoid cells. Although IL-35 was only one of several different EV-based components (e.g., CD39 and CD73) mediating primary suppression, the passive uptake of IL-35 subunits and IL-35 reexpression at the cell surface, coupled with the ability of p35 and Ebi3 subunits to co-localize and chronically associate upon reaching the cell surface, endowed IL-35 with unique secondary suppressive capacities: (1) the suppression of naive T cells by contact with IL-35-EV-altered lymphocytes and (2) exhaustion of the latter by chronic formation of IL-35 on the cell surface and self-stimulation via IL-35 receptors.

The EV method of delivery of IL-35 we observed throughout these studies does not appear unique to the CBA to B6 tolerance model using DST and anti CD154, as the use of a 2W1S-tolerization protocol in B6 mice (Young et al., 2018) showed that any peptide-specific $CD4^+$ T cell could become a tolerogenic agent of IL-35 EV production (Figure S6). The role of IL-35 in primary suppression of T cell responses appears redundant, as the use of EVs from CBA-tolerized, Treg-cell-specific Ebi3-KO mice had similar suppressive effects on graft survival in a murine allo-heart transplantation model (Figure 5D). Similarly, Treg cell EVs from both $Treg^{Ebi3WT}$ and $Treg^{Ebi3KO}$, CBA-tolerized mice suppressed tvDTH responses to TT equally well, consistent with the known primary immunosuppressive properties of Treg-cell-derived exosomes (Okoye et al., 2014; Smyth et al., 2013). However, the role of EV-IL-35 in secondary suppression was without compensatory mechanisms and is likely unique to this cytokine.

Typically, cytokines are believed to be produced by one cell and act through a single receptor-binding event upon another cell to elicit an observed effect, consistent with the function of a well-described suppressive cytokine, IL-10. Other suppressive cytokines, such as TGF-β, display a pattern of activity wherein the cytokine is expressed latently on the surface of the producing cell and requires physical contact and enzymatic cleavage to release the latency component (LAP) and liberate active TGF-β, which then proceeds to bind its receptor and mediate suppression. Our data strongly support the idea that IL-35 is an atypical cytokine in that both of the subunits that comprise IL-35, Ebi3, and p35 were

secreted in $CD81^+$ EVs and acted either directly (primary suppression) or indirectly (secondary suppression), the latter by altering the target cell through a system of EV uptake and reexpression (Figure 6). This unique production and delivery of IL-35 was unlike that of IL-10, which is reported to be produced in reciprocal fashion by Treg cells (Sawant et al., 2019). Our observation that IL-35 is produced in vesicular rather than H_2O-soluble form (Figures S1B and S1C) makes it quite different from other members of the IL-12 family and likely accounts for the difficulty in producing a stable, double-chain, bioactive cytokine (Aparicio-Siegmund et al., 2014). While we cannot at this time rule out the possibility that the Ebi3 or p35 present on the EV is binding sequentially to the appropriate subunit of the IL-35 receptor on the acquiring cell to form active IL-35, it would appear that the vast majority of IL-35 components carried by $CD81^+$ EVs are not closely associated, maintaining the IL-35 in a relatively inactive state. However, depending on the local concentration of the two components, a stable dimer of Ebi3/p35 may form. The rare event of IL-35 components reassociating after the EV is endocytosed, fused to the recipient cell's internal membrane, and delivered to the cell surface thus becomes a unique pathway to infectious peripheral tolerance. A similar use of CD81 to gain entry into a cell has been reported to be necessary for infection of hepatocytes by hepatitis C virus, which is released in the acid environment of the late endosome due to a pH-dependent structural change opening the CD81 large extracellular loop (Cunha et al., 2017).

The effect of IL-35 in suppressing cell-mediated immunity has been shown in various immunological responses, including those in the tumor microenvironment, viral infection, and transplantation as well as in immune responses to self-proteins. Consistent with the report on tumor-infiltrating T cells by Turnis et al. (2016), we observed an increase in exhaustion-related proteins, including LAG-3, TIM-3, and PD-1, in T and B cells following tolerance induction. However, rather than affecting the entire lymphocyte population, the phenotype of elevated IRs was entirely restricted to the IL-35 EV-acquiring T cells and B cells. Exactly how IL-35-mediated exhaustion occurs is not entirely clear. One possibility is that the IL-35 formed at the cell surface by transient, polarized association of tetraspanin associated subunits might act in *cis* to repeatedly stimulate the IL-35R (gp130/IL-12Rβ2 complex) on the surface of the same EV-acquiring cell (Figure 6). Such repeated "self"-stimulation might force the change to an exhaustion phenotype. The restricted tetraspanin use by lymphoid cells producing IL-35 EVs may be relevant here; for example, in contrast to CD81, CD9, the tetraspanin previously associated with DC-derived EVs in maternal-fetal tolerance (Bracamonte-Baran et al., 2017), was not detected in association with p35 and $Ebi3^+$ EVs (Figure 4H).

Once the Treg-cell-derived EV reaches its target cell, several rapid primary suppressive effects may occur, including inhibition of proliferation (Aiello et al., 2017), blockage of TNF-α and interferon-γ (IFN-γ) cytokine secretion mediated by EV miRNA cargo (Okoye et al., 2014), curtailed cytotoxicity (Szczepanski et al., 2011), and tvDTH inhibition (Figure 5). In addition, we found an infectious component, the development of secondary suppressive effects related to acquisition and stable surface display of the acquired IL-35 cytokines by EV-altered T (or B) bystander cells (Figures 1D, 2C, 3C, and S5D; modeled in Figure 6).

In conclusion, we have shown the suppression of T cell responses by IL-35 through an EV-mediated “infectious tolerance” mechanism. This mechanism appears to be useful in propagating tolerance; besides primary immunosuppression, the IL-35^{+} EV-mediated secondary suppression adds a role for bystander, EV-acquiring cells to be used as agents of tolerance simply by passively acquiring EVs and then interacting with other cells. Indeed by day 35 of tolerance induction, the infectious aspect of IL-35 EVs had spread tolerance far beyond the initiating Treg cell, such that the majority of IL-35 was now produced by non-Treg cells (Figure S1C; Collison et al., 2010). Just as EVs from donor DC have been shown to amplify allo-sensitization in graft recipients leading to acute rejection, our findings suggest that Treg cell EV-dependent mechanisms of tolerance amplification could be exploited clinically to target delivery of immunosuppressive agents such as IL-35 in transplant or autoimmune treatment protocols.

STAR★METHODS

LEAD CONTACT AND MATERIALS AVAILABILITY

Further information and requests for resources and reagents should be directed to and will be fulfilled by the Lead Contact, Jeremy Sullivan (sullivan@surgery.wisc.edu). This study did not generate new unique reagents.

EXPERIMENTAL MODEL AND SUBJECT DETAILS

Mice—Both male and nulliparous female mice used throughout this study were bred and maintained at animal facilities at the University of Wisconsin-Madison according to specific pathogen free conditions. All animal care and handling were performed under IACUC institutional guidelines in accordance with IACUC protocol number M00604. C57 BL/6 (B6) [H2^{b}], CBA/J (CBA) [H2^{k}], DBA/2 [H2^{d}], Ebi3^{ko} (B6.129X1-Ebi3^{tm1Rsb}/J) and Thy1.1 C57 BL/6 (Thy 1.1 B6) [PL-Thy 1a/CyJ; H2^{b}], mice were purchased from Harlan Sprague Dawley (Indianapolis, IN, USA) or Jackson Labs (Bar harbor, ME, USA). We used a two types of double reporter transgenic mice (C57BL/6; H2^{b} background): 1) ones which expressed YFP under the *Foxp3* and Td^{Tom} under the *Ebi3* promoter [Foxp3$^{Cre\text{-}YFP}$.Ebi3$^{Cre\text{-}tdTom}$] (Treg^{Ebi3WT}), and 2) ones in which both reporters were present, but Ebi3 protein was selectively knocked out in Foxp3^{+} cells [*Foxp3*^{CreYFP}.*Ebi3*^{Floxed}], (Treg^{Ebi3KO}), both kindly provided by Dario Vignali (University of Pittsburgh). Reporter expression was confirmed by flow cytometry. We chose to use tolerance induction by DST and anti-CD154 monoclonal antibody, as a means of analyzing our hypothesis.

Tolerance induction and allogeneic re-challenge *in vitro*—Tolerance induction by DST plus anti-CD40L treatment of C57BL/6 mice was described previously (Tomita et al., 2016). For allogeneic re-challenge, 1.0 × 10^{6} cells/well of lymph node cells harvested from tolerized Treg^{Ebi3WT} and Treg^{Ebi3KO} B6 mice were co-cultured with complete media plus 10% heat inactivated FBS (200 μL/well) and each antigen; B6 [syngeneic-], CBA [allogeneic-], or DBA/2 [3rd party-] cell lysate (10 μg/well) in a 96-well plate for 24 hours at 37°C and 5% CO_2. After 24 hours, cells were harvested, washed, stained, fixed, and analyzed with BD FACS LSRII and/or the Amnis-ImageStream imaging cytometer.

METHOD DETAILS

Standard and imaging flow cytometry—Standard: Fluorochrome-labeled monoclonal anti-mouse antibodies were used at proper concentrations according to vendor technical documents and/or titration experiments in our lab. Cells were stained in 2% BSA-PBS with anti-p35, Ebi3, CD4, CD3, CD25, and appropriate secondary antibody for no more than 60 minutes on ice in the dark. Cells were washed twice with 2%BSA-PBS and fixed in 2% Paraformaldehyde until standard or imaging flow cytometry experiments could be performed.

Imaging Flow Cytometry: Immunostaining of mouse samples was performed in the same way as described above. A two-laser ImageStream® Amnis device was used (4 channels plus Brightfield and 40X or 60X) for imaging flow detection. In certain experiments, channel 6 (762/35) was used as an extra fluorescent channel (blue laser) instead of side-scatter (red laser). All images were acquired at 60X magnification. Analysis was performed using the software Ideas® version 6.0 by Amnis.

EV isolation and analysis—EVs were isolated from spleen of tolerized B6 mice by culturing splenocytes with complete media plus 10% heat inactivated EV-depleted FBS and allo-specific CBA or 3rd party DBA cell lysate for 24 hours at 37°C and 5% CO_2. The supernatants were collected and subjected to serial centrifugation at 4°C, 300xg for 10 minutes (removing cells), 2,000xg for 10 minutes (removing dead cells) and 10,000xg for 30 minutes (removing cell debris). After that, supernatants were filtered (0.45um) and subjected to 100,000xg ultra-centrifugation for 2 hours at 4°C. Supernatants were collected as an EV-free fraction, and the pellets were re-suspended in 4mLs of PBS (Thery et al., 2006). We then performed another 100,000xg ultra-centrifugation for 2 hours at 4°C. Finally, the EVs were re-suspended in 50 μLs of PBS. Protein concentration in the preparation was performed using a nano-drop spectrophotometer (280nm). Isolated EVs were analyzed by transmission electro-microscopy, NTA analysis, ELISA and Western Analysis.

ELISA

The ELISA assay for extracellular vesicle-associated IL35 was done using a modification of the method of Logozzi et al. (2009). Half-area-well microtiter plates were coated with various capture antibodies at 10 ug/ml each in 10 mM TRIS (pH 9) and incubated overnight at 4°C. After blocking plate in 2% bovine serum albumin in PBS for 3 hours at room temperature, tested samples were added and plates were incubated overnight at 4°C. Wells were washed and bound target antigen was detected with biotinylated anti-tetraspanin monoclonal antibodies (either anti-CD81 (Thermo Fisher, MA5-17938), or anti-CD9 (Biolegend, MZ3) at 1ug/ml concentration. After 3 hours of incubation at room temperature, wells were washed and solution containing HRP-conjugated avidin was added at 1:1000 dilution. After 45 min incubation, wells were washed and a solution containing TMB was added. The enzyme reaction was stopped after 5-10 minutes with TMB stop solution. Color development was read at 450 nm.

Immunoprecipitation and western analysis—Isolated EV solutions (20 μg) were boiled in loading buffer containing sample buffer and RIPA lysis buffer, and electrophoresed

on a 4%–20% Mini-Protein TGX Precast Gels (BioRad) without β-Mercapto-ethanol. After transferring, proteins were blocked in 5% BSA for 1 hour at room temperature. The membrane were incubated with primary antibodies of anti-CD81 (1:200; EAT-2), anti-p35 (1:200; 45806), anti-Ebi3 (1:400; V1.4H6.29) for overnight at 4°C, and then with 1:3000 diluted HRP-conjugated secondary antibodies for 1 hour at room temperature. We visualized the target molecule using a Las-4000 mini imager. Immunoprecipitation studies were done using cyanogen-bromide-activated Sepharose 4B beads were coupled to either anti-Ebi3 antibody (DV29) or anti-p35 antibody (clone # 45806, R&D Systems) to achieve a concentration of 2 mg of antibody per ml of swollen beads. Antibody binding efficiency was corroborated by determination of the protein concentration before and after overnight incubation with swollen beads. Then, the beads were blocked by incubation with 1 ethanolamine followed by two washes with PBS and three washes with alternating cycles of 0.1M borate/0.5 M NaCl pH 8.0 and 0.1 acetate/0.5 M NaCl pH 4.0. 25 uls of antibody-coupled bead slurry were incubated with EV samples overnight at 4 C with tilting and rotation. The supernatant was collected, and the beads washed 3x with PBS-Tween 0.05%. Beads were subsequently re-suspended in SDS-PAGE sample buffer (containing 2% SDS, EDTA but no β-mercapto-ethanol) and heated to 100°C before proceeding to SDS-PAGE.

Transwell assay—Lymphocytes were isolated from spleens and lymph nodes of Thy 1.2^+ $Treg^{Ebi3WT}$ (*Foxp3*$^{Cre\text{-}YFP}$.*Ebi3*^{tdTom}) mice on day 35 after tolerization or $Ebi3^{KO}$ mice. 3.0×10^6 cells/well of the lymph node cells were co-cultured with complete media plus 10% heat inactivated EV-depleted FBS (600 μL/well) and allo-specific CBA cell lysate (30 μg/well) in the 1.0 micron transwell culture system. In order to assess surface $Ebi3^+$ cells transfer efficiency in Treg cell EV, lymph node cells harvested from untreated Thy 1.1 B6 mice (bottom) were cultured separated from those from tolerized Thy1.2 B6 mice (top) by 1.0 μm pore transwell inserts (Corning) for 24 hours at 37°C and 5% CO_2 in a 24-well plate. Then, the cells on each well were harvested, washed, stained, fixed, and the proportion of transferred surface $Ebi3^+$ $CD4^+$ T cells analyzed with BD FACS LSRII and ImageStream.

EV co-culture and secondary immune suppression assay—Either 1.0×10^6 cells/well of LNC, or of purified T cells harvested from naive B6 mice were co-cultured in complete media plus 10% heat inactivated EV-depleted FBS (200 μL/well) with purified EV from CBA-stimulated, tolerized B6 mouse spleen cells (20 μg/well) in a 96-well plate. After 24 hours at 37°C and 5% CO_2, cells were harvested, washed, stained, fixed, and analyzed with BD FACS LSRII and ImageStream. For secondary suppression experiments, naive B6 cells treated with EV harvested from cultures of tolerized, $Treg^{Ebi3KO}$ (IL35-deficient) SC were compared with B6 cells treated with EV from cultures of tolerized, $Treg^{Ebi3WT}$ (IL35-sufficient) SC for their ability to suppress a TT-specific tvDTH response. EV-modified cells were mixed with $4x10^6$ TT-sensitized SC at varying ratio, with naive B6 cells were added so that the final injected cell number remained constant ($8x10^6$).

Trans-vivo Delayed Type Hypersensitivity assay (tvDTH assay)—Allo-antigens were prepared as follows: $1.0\ x10^7$ splenocytes of B6, CBA, or DBA/2 were washed twice in sterile PBS, and re-suspended in 0.1 mL PBS containing 10 μg/mL phenylmethylsulfonyl fluoride (Sigma-Aldrich). The cells were then sonicated using a VR50 sonicator fitted with a

2-mmprobe (Sonics). The disrupted cells were centrifuged for 30 min at 14,000 g at 4°C to remove debris. The protein content of the supernatant was determined using a micro BCA Protein Assay kit (Pierce). A total of 20 μg of protein was used for each injection in the DTH assays and referred to as either B6 [syngeneic/self], CBA [allogeneic/donor], or DBA/2 [3rd party] antigen. Responder cells were prepared as follows: At the time points indicated, tolerized mice were euthanized and spleen harvested. With recovered splenocytes, we injected 1.0 $x10^7$ cells from treated mice into syngeneic (B6) naive mice footpads with either: PBS [negative control], TT/DT recall antigen (25 μg) [positive control], test antigen (20 μg) [B6, CBA, or DBA/2 cell lysate], or a combination of TT/DT and test antigen [for linked suppression determination]. Before injection and after 24 hours, we used a dial-thickness gauge to measure footpad thickness; change in thickness, after subtraction of PBS value [net swelling] was expressed in units of $1.0x10^{-4}$ inches. To determine the extent of "linked suppression" we used the following formula:

$$\% \text{ Inhibition} = 1 - ((\text{TT plus antigen}) \text{ response} \ / \ \text{TT response}) x100$$

comparing the footpad swelling response to TT/DT recall antigen alone, with the response to the combination of TT/DT and test antigen. The results were expressed as % inhibition of the recall response. When the % inhibition value with syngeneic antigen was equal or greater than the % inhibition value with allogeneic-antigen, we considered the regulation in the mouse to be entirely nonspecific. When the % inhibition value with syngeneic antigen was less than the % inhibition value with allogeneic-antigen, we considered this to be evidence of allo-specific regulation. All corrected tvDTH values used to calculate % inhibition represent the observed tvDTH response for the respective group minus the PBS control. Co-injected blocking antibodies were used at either 10 μg/injection (αTGFβ, αIL10, αIL4) or 1 μg/injection (αIL12-p35 or αEbi3).

Heart transplantation—Heart transplantations were performed using a modification of the protocol by Corry et al. (1973). Briefly, recipient mice were anesthetized with isoflurane, shaved and cleansed with 70% ethanol. Proximal and distal ties with 6-0 silk were placed around the aorta and vena cava in preparation for later occlusion. A midline abdominal incision was made in the donor animal and a 10% heparin solution in saline was injected into the inferior vena cava. Under 16X magnification the inferior vena cava was ligated with 6-0 silk and divided inferior to the tie. The superior vena cava was similarly ligated and divided superior to the tie. After blood was evacuated from the heart, a ligature was placed around the pulmonary veins, which were divided distal to the ligature. The heart was lifted from the chest and placed in chilled Ringer's lactate solution.

The recipient, under microscope, was clamped around the aorta and vena cava. The donor heart was removed from chilled solution, and donor aorta and pulmonary artery were joined end-to-side to the recipient aorta and vena cava. After completion of anastomoses a thin layer of gelfoam was added. Upon release of the proximal occluding clamp of the aorta and coronary arteries, the transplant was perfused with oxygenated recipient blood. The animals were allowed to recover under a heat lamp with supervision. On the same day of

transplantation, CBA recipient mice were administrated PBS or 20 μg (protein) EV purified from B6 mice by intravenous injection.

Transmission electron microscopy – Negative Staining and Immuno-gold labeling—Isolated EVs were fixed in 2% paraformaldehyde-1% glutaraldehyde solution for one hour. 5 ul additions of EVs were added to 300-mesh carbon/formvar coated copper grids. Quenched grids were blocked with 1% BSA and stained with a combination of anti-IL35 (1:200; Shenandoah Biotech, DV29), anti-p35 (1:100; R&D Systems, MAB6688) or anti-CD81 (1:100; Cell Signaling Technology, D5O2Q) overnight at 4°C. Stained grids were then incubated with the appropriate secondary antibody conjugated gold bead of either 15nm (CD81), 10nm (Ebi3) or 6nm (p35) at room temperature for 1 hour. Grids were washed multiple times, fixed in 1% glutaraldehyde, exposed to 3% uranyl acetate for 20 s and dried before viewing on FEI Tecnai T-12 transmission electron microscope.

Particle size and concentration analysis- Nanoparticle Tracking Analysis (NTA)—The size distribution and particle concentration of the isolated EVs were measured using a Nanosight NS300 equipped with Nanosight NTA 3.3 software and 488 nm laser (Malvern Instruments, UK). 5 videos of 60 s each were recorded for all EV samples at camera level 12 and syringe pump speed of 70. The analysis was done at 25 frames/sec with detection threshold of 3. All samples were diluted to appropriate concentration in PBS prior to measurement.

QUANTIFICATION AND STATISTICAL ANALYSIS

Statistical analyses were performed by Graph pad Prism (GraphPad Software v 5.01, San Diego, CA). The p values were calculated using Mann-Whitney U tests. Heart graft survival estimation was analyzed using the Kaplan-Meier method. Differences in the survival rates between groups were assessed by the log-rank test. $p < 0.05$ was considered to indicate a significant difference.

DATA AND CODE AVAILABILITY

This study did not generate any unique datasets or code.

Supplementary Material

Refer to Web version on PubMed Central for supplementary material.

ACKNOWLEDGMENTS

We wish to thank Dagna Sheerar and the personnel of the UW Carbone Cancer Center Flow Laboratory for technical support on flow cytometry and Image Stream experiments. We also acknowledge the support of Dr. Anita Chong and Dr. Marisa Alegre and their labs at the University of Chicago for providing splenocytes from BALB/c × C57BL/6 [Tg for mOVA-2W1S] mice for tolerization studies and Scott Burlingham for discussion and suggestions. This project was supported by the NIH (grant R01-AI119140-03 to W.J.B., R03-144-AAH5568 to J.A.S. and grants R01 CA203689 and P30 CA047904 to D.A.A.V.) and University of Wisconsin Carbone Cancer Center (support grant P30 CA014520).

REFERENCES

Abbas AK, Benoist C, Bluestone JA, Campbell DJ, Ghosh S, Hori S, Jiang S, Kuchroo VK, Mathis D, Roncarolo MG, et al. (2013). Regulatory T cells: recommendations to simplify the nomenclature. Nat. Immunol 14, 307–308. [PubMed: 23507634]

Agarwal A, Fanelli G, Letizia M, Tung SL, Boardman D, Lechler R, Lombardi G, and Smyth LA (2014). Regulatory T cell-derived exosomes: possible therapeutic and diagnostic tools in transplantation. Front. Immunol 5, 555. [PubMed: 25414702]

Aiello S, Rocchetta F, Longaretti L, Faravelli S, Todeschini M, Cassis L, Pezzuto F, Tomasoni S, Azzollini N, Mister M, et al. (2017). Extracellular vesicles derived from T regulatory cells suppress T cell proliferation and prolong allograft survival. Sci. Rep 7, 11518. [PubMed: 28912528]

Aparicio-Siegmund S, Moll JM, Lokau J, Grusdat M, Schröder J, Plöhn S, Rose-John S, Grötzinger J, Lang PA, Scheller J, and Garbers C (2014). Recombinant p35 from bacteria can form Interleukin (IL-)12, but Not IL-35. PLoS ONE 9, e107990. [PubMed: 25259790]

Bettini M, Castellaw AH, Lennon GP, Burton AR, and Vignali DA (2012). Prevention of autoimmune diabetes by ectopic pancreatic β-cell expression of interleukin-35. Diabetes 61, 1519–1526. [PubMed: 22427377]

Bracamonte-Baran W, Florentin J, Zhou Y, Jankowska-Gan E, Haynes WJ, Zhong W, Brennan TV, Dutta P, Claas FH, van Rood JJ, and Burlingham WJ (2017). Modification of host dendritic cells by microchimerism-derived extracellular vesicles generates split tolerance. Proc. Natl. Acad. Sci. USA 114, 1099–1104. [PubMed: 28096390]

Burrell BE, and Bromberg JS (2012). Fates of CD4+ T cells in a tolerant environment depend on timing and place of antigen exposure. Am. J. Transplant 12, 576–589. [PubMed: 22176785]

Collison LW, Workman CJ, Kuo TT, Boyd K, Wang Y, Vignali KM, Cross R, Sehy D, Blumberg RS, and Vignali DA (2007). The inhibitory cytokine IL-35 contributes to regulatory T-cell function. Nature 450, 566–569. [PubMed: 18033300]

Collison LW, Chaturvedi V, Henderson AL, Giacomin PR, Guy C, Bankoti J, Finkelstein D, Forbes K, Workman CJ, Brown SA, et al. (2010). IL-35-mediated induction of a potent regulatory T cell population. Nat. Immunol 11, 1093–1101. [PubMed: 20953201]

Corry RJ, Winn HJ, and Russell PS (1973). Primarily vascularized allografts of hearts in mice. The role of H-2D, H-2K, and non-H-2 antigens in rejection. Transplantation 16, 343–350. [PubMed: 4583148]

Cunha ES, Sfriso P, Rojas AL, Roversi P, Hospital A, Orozco M, and Abrescia NGA (2017). Mechanism of structural tuning of the hepatitis C virus human cellular receptor CD81 large extracellular loop. Structure 25, 53–65. [PubMed: 27916518]

Devergne O, Hummel M, Koeppen H, Le Beau MM, Nathanson EC, Kieff E, and Birkenbach M (1996). A novel interleukin-12 p40-related protein induced by latent Epstein-Barr virus infection in B lymphocytes. J. Virol 70, 1143–1153. [PubMed: 8551575]

Dixon KO, van der Kooij SW, Vignali DA, and van Kooten C (2015). Human tolerogenic dendritic cells produce IL-35 in the absence of other IL-12 family members. Eur. J. Immunol 45, 1736–1747. [PubMed: 25820702]

Geissler EK (2012). The ONE Study compares cell therapy products in organ transplantation: introduction to a review series on suppressive monocyte-derived cells. Transplant. Res 1, 11. [PubMed: 23369457]

Graca L, Cobbold SP, and Waldmann H (2002). Identification of regulatory T cells in tolerated allografts. J. Exp. Med 195, 1641–1646. [PubMed: 12070291]

Jankowska-Gan E, Sheka A, Sollinger HW, Pirsch JD, Hofmann RM, Haynes LD, Armbrust MJ, Mezrich JD, and Burlingham WJ (2012). Pretransplant immune regulation predicts allograft outcome: bidirectional regulation correlates with excellent renal transplant function in living-related donor-recipient pairs. Transplantation 93, 283–290. [PubMed: 22186938]

Kosaka N, Iguchi H, Yoshioka Y, Takeshita F, Matsuki Y, and Ochiya T (2010). Secretory mechanisms and intercellular transfer of microRNAs in living cells. J. Biol. Chem 285, 17442–17452. [PubMed: 20353945]

Li W, Bribriesco AC, Nava RG, Brescia AA, Ibricevic A, Spahn JH, Brody SL, Ritter JH, Gelman AE, Krupnick AS, et al. (2012). Lung transplant acceptance is facilitated by early events in the graft and is associated with lymphoid neogenesis. Mucosal Immunol. 5, 544–554. [PubMed: 22549742]

Li J, Liu K, Liu Y, Xu Y, Zhang F, Yang H, Liu J, Pan T, Chen J, Wu M, et al. (2013). Exosomes mediate the cell-to-cell transmission of IFN-α-induced antiviral activity. Nat. Immunol 14, 793–803. [PubMed: 23832071]

Liu Q, Rojas-Canales DM, Divito SJ, Shufesky WJ, Stolz DB, Erdos G, Sullivan ML, Gibson GA, Watkins SC, Larregina AT, and Morelli AE (2016). Donor dendritic cell-derived exosomes promote allograft-targeting immune response. J. Clin. Invest 126, 2805–2820. [PubMed: 27348586]

Logozzi M, De Milito A, Lugini L, Borghi M, Calabrò L, Spada M, Perdicchio M, Marino ML, Federici C, Iessi E, et al. (2009). High levels of exosomes expressing CD63 and caveolin-1 in plasma of melanoma patients. PLoS ONE 4, e5219. [PubMed: 19381331]

Marino J, Babiker-Mohamed MH, Crosby-Bertorini P, Paster JT, Le-Guern C, Germana S, Abdi R, Uehara M, Kim JI, Markmann JF, et al. (2016). Donor exosomes rather than passenger leukocytes initiate alloreactive T cell responses after transplantation. Sci. Immunol 1, 1–10.

Niedbala W, Wei XQ, Cai B, Hueber AJ, Leung BP, McInnes IB, and Liew FY (2007). IL-35 is a novel cytokine with therapeutic effects against collagen-induced arthritis through the expansion of regulatory T cells and suppression of Th17 cells. Eur. J. Immunol 37, 3021–3029. [PubMed: 17874423]

Okoye IS, Coomes SM, Pelly VS, Czieso S, Papayannopoulos V, Tolmachova T, Seabra MC, and Wilson MS (2014). MicroRNA-containing T-regulatory-cell-derived exosomes suppress pathogenic T helper 1 cells. Immunity 41, 89–103. [PubMed: 25035954]

Olson BM, Jankowska-Gan E, Becker JT, Vignali DA, Burlingham WJ, and McNeel DG (2012). Human prostate tumor antigen-specific CD8+ regulatory T cells are inhibited by CTLA-4 or IL-35 blockade. J. Immunol 189, 5590–5601. [PubMed: 23152566]

Olson BM, Sullivan JA, and Burlingham WJ (2013). Interleukin 35: a key mediator of suppression and the propagation of infectious tolerance. Front. Immunol 4, 315. [PubMed: 24151492]

Park AC, Huang G, Jankowska-Gan E, Massoudi D, Kernien JF, Vignali DA, Sullivan JA, Wilkes DS, Burlingham WJ, and Greenspan DS (2015). Mucosal administration of collagen V ameliorates atherosclerotic plaque burden by inducing IL-35-dependent tolerance. J. Biol. Chem 291, 3359–3370. [PubMed: 26721885]

Qin S, Cobbold SP, Pope H, Elliott J, Kioussis D, Davies J, and Waldmann H (1993). "Infectious" transplantation tolerance. Science 259, 974–977. [PubMed: 8094901]

Rosenblum MD, Gratz IK, Paw JS, Lee K, Marshak-Rothstein A, and Abbas AK (2011). Response to self antigen imprints regulatory memory in tissues. Nature 480, 538–542. [PubMed: 22121024]

Sanchez Rodriguez R, Pauli ML, Neuhaus IM, Yu SS, Arron ST, Harris HW, Yang SH, Anthony BA, Sverdrup FM, Krow-Lucal E, et al. (2014). Memory regulatory T cells reside in human skin. J. Clin. Invest 124, 1027–1036. [PubMed: 24509084]

Sawant DV, Yano H, Chikina M, Zhang Q, Liao M, Liu C, Callahan DJ, Sun Z, Sun T, Tabib T, et al. (2019). Adaptive plasticity of IL-10^{+} and IL-35^{+} T_{reg} cells cooperatively promotes tumor T cell exhaustion. Nat. Immunol 20, 724–735. [PubMed: 30936494]

Shen P, Roch T, Lampropoulou V, O'Connor RA, Stervbo U, Hilgenberg E, Ries S, Dang VD, Jaimes Y, Daridon C, et al. (2014). IL-35-producing B cells are critical regulators of immunity during autoimmune and infectious diseases. Nature 507, 366–370. [PubMed: 24572363]

Smyth LA, Ratnasothy K, Tsang JY, Boardman D, Warley A, Lechler R, and Lombardi G (2013). CD73 expression on extracellular vesicles derived from CD4+ CD25+ Foxp3+ T cells contributes to their regulatory function. Eur. J. Immunol 43, 2430–2440. [PubMed: 23749427]

Sullivan JA, Adams AB, and Burlingham WJ (2014). The emerging role of TH17 cells in organ transplantation. Transplantation 97, 483–489. [PubMed: 24212502]

Sullivan JA, Jankowska-Gan E, Hegde S, Pestrak MA, Agashe VV, Park AC, Brown ME, Kernien JF, Wilkes DS, Kaufman DB, et al. (2017). Th17 responses to collagen type V, kα1-tubulin, and vimentin are present early in human development and persist throughout life. Am. J. Transplant 17, 944–956. [PubMed: 27801552]

Szczepanski MJ, Szajnik M, Welsh A, Whiteside TL, and Boyiadzis M (2011). Blast-derived microvesicles in sera from patients with acute myeloid leukemia suppress natural killer cell function via membrane-associated transforming growth factor-beta1. Haematologica 96, 1302–1309. [PubMed: 21606166]

Takasato F, Morita R, Schichita T, Sekiya T, Morikawa Y, Kuroda T, Niimi M, and Yoshimura A (2014). Prevention of allogeneic cardiac graft rejection by transfer of ex vivo expanded antigen-specific regulatory T-cells. PLoS ONE 9, e87722. [PubMed: 24498362]

Tedder TF, and Leonard WJ (2014). Autoimmunity: regulatory B cells–IL-35 and IL-21 regulate the regulators. Nat. Rev. Rheumatol 10, 452–453. [PubMed: 24934192]

Terayama H, Yoshimoto T, Hirai S, Naito M, Qu N, Hatayama N, Hayashi S, Mitobe K, Furusawa J, Mizoguchi I, et al. (2014). Contribution of IL-12/IL-35 common subunit p35 to maintaining the testicular immune privilege. PLoS ONE 9, e96120. [PubMed: 24760014]

Thery C, Amigorena S, Raposo G, and Clayton A (2006). Isolation and characterization of exosomes from cell culture supernatants and biological fluids. Curr. Protoc. Cell Biol Chapter 3, Unit 3.22.

Todo S, Yamashita K, Goto R, Zaitsu M, Nagatsu A, Oura T, Watanabe M, Aoyagi T, Suzuki T, Shimamura T, et al. (2016). A pilot study of operational tolerance with a regulatory T-cell-based cell therapy in living donor liver transplantation. Hepatology 64, 632–643. [PubMed: 26773713]

Tomita Y, Satomi M, Bracamonte-Baran W, Jankowska Gan E, Workman AS, Workman CJ, Vignali DA, and Burlingham WJ (2016). Kinetics of alloantigen-specific regulatory CD4 T cell development and tissue distribution after donor-specific transfusion and costimulatory blockade. Transplant. Direct 2, e73. [PubMed: 27500263]

Turnis ME, Sawant DV, Szymczak-Workman AL, Andrews LP, Delgoffe GM, Yano H, Beres AJ, Vogel P, Workman CJ, and Vignali DA (2016). Interleukin-35 limits anti-tumor immunity. Immunity 44, 316–329. [PubMed: 26872697]

Vaidyanathan H, Zhou Y, Petro TM, and Schwartzbach SD (2003). Intracellular localization of the p35 subunit of murine IL-12. Cytokine 21, 120–128. [PubMed: 12697150]

Wang Z, Liu JQ, Liu Z, Shen R, Zhang G, Xu J, Basu S, Feng Y, and Bai XF (2013). Tumor-derived IL-35 promotes tumor growth by enhancing myeloid cell accumulation and angiogenesis. J. Immunol 190, 2415–2423. [PubMed: 23345334]

Wang RX, Yu CR, Dambuza IM, Mahdi RM, Dolinska MB, Sergeev YV, Wingfield PT, Kim SH, and Egwuagu CE (2014). Interleukin-35 induces regulatory B cells that suppress autoimmune disease. Nat. Med 20, 633–641. [PubMed: 24743305]

Warren KJ, Iwami D, Harris DG, Bromberg JS, and Burrell BE (2014). Laminins affect T cell trafficking and allograft fate. J. Clin. Invest 124, 2204–2218. [PubMed: 24691446]

Young JS, Yin D, Vannier AGL, Alegre ML, and Chong AS (2018). Equal expansion of endogenous transplant-specific regulatory T cell and recruitment into the allograft during rejection and tolerance. Front. Immunol 9, 1385 [PubMed: 29973932]

Highlights

- IL-35 subunits Ebi3 and p35 are secreted as components of $CD81^+$ EVs
- $IL\text{-}35^+$ EVs secreted by a small number of Treg cells target a higher number of lymphocytes
- EV coating of bystander lymphocytes with IL-35 promotes infectious tolerance

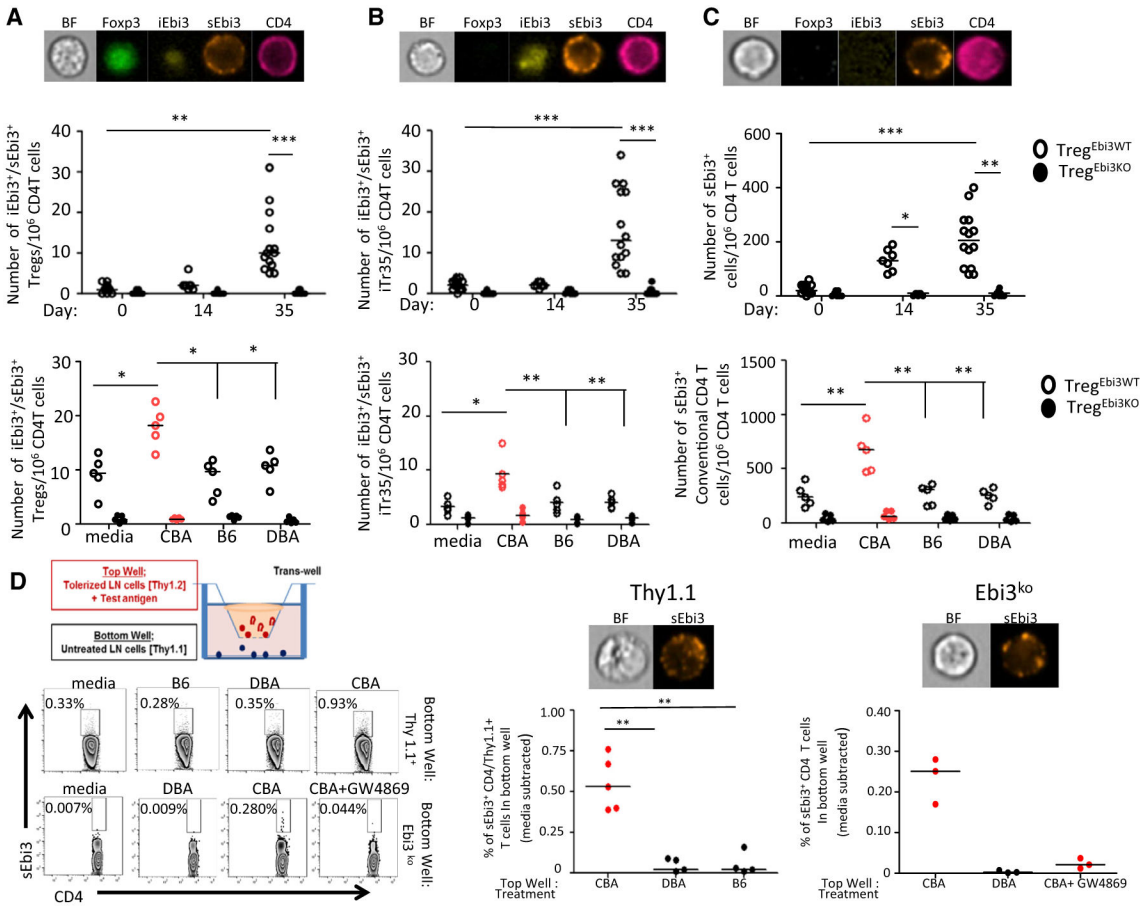

Figure 1. Endogenous Production of Surface-Bound Ebi3 (sEbi3) by Allo-Specific Treg or iTr35 Cells and the Acquisition of sEbi3 by Conventional Effector CD4$^+$ T Cells

The analysis of cell types shown in (A)–(C) is similar. An image of each cell type (top), the kinetics of its appearance (middle), and a summary of *in vitro* restimulation with various antigens on day 35 (bottom) are shown.

(A) Top: representative imaging flow cytometry example showing the staining pattern for sEbi3 on a Treg cell (Foxp3$^+$) that produces Ebi3 (iEbi3$^+$) following CBA + anti-CD154 tolerization protocols. Middle: graph indicating the total number of Treg^{Ebi3WT} CD4$^+$ T cells that express surface Ebi3 (open circle) at three time points; these Treg cells were significantly increased at 35 days post-tolerization initiation as compared to Treg^{Ebi3KO} mice (closed circle). Bottom: overnight stimulation with indicated antigen of day 35 CBA-tolerized reporter mice shows that CBA stimulation caused a significant increase in the number of Treg^{Ebi3WT} CD4$^+$ T cells that express surface Ebi3 by conventional flow cytometry.

(B) Top: representative imaging flow cytometry example showing the staining pattern for sEbi3 on a iTr35 CD4$^+$ (Foxp3^{neg}) T cells that produced Ebi3 (iEbi3$^+$) following CBA + anti-CD154 tolerization protocols. Middle: graph indicating the total number of Treg^{Ebi3WT} CD4$^+$ T cells that express sEbi3 (open circle) were significantly increased at 35 days following CBA + anti-CD154 tolerization versus tolerized Treg^{Ebi3KO} (closed circle) controls as assessed by flow cytometry. Bottom: overnight stimulation with indicated antigen

of day 35 CBA-tolerized reporter mice shows that CBA stimulation caused a significant increase in the number of $Treg^{Ebi3WT}$ iTr35 $CD4^+$ T cells that express surface Ebi3 by conventional flow cytometry. Overnight stimulation with indicated antigen of day 35 CBA-tolerized reporter mice shows that CBA restimulation causes a significant increase in the number of $Treg^{Ebi3WT}$ iTr35 $CD4^+$ T cells that express surface Ebi3 by conventional and imaging flow cytometry, whereas iT35 cells from tolerized $Treg^{Ebi3KO}$ remain sEbi3 negative (bottom).

(C) Top: representative imaging flow cytometry staining of sEbi3 on a non-Treg, non-Ebi3-producing $CD4^+$ T cell after tolerization. Middle: the amount of $CD4^+$ T cells negative for both Foxp3Cre-YFP and Ebi3tdTom that expressed surface Ebi3 was also quantified over time, showing a marked increase detectable on day 14. Bottom: overnight CBA restimulation of LNCs from day-35-tolerized mice shows an antigen-specific increase in the number of $sEbi3^+$ but $Foxp3^{neg}$ and $iEbi3^{neg}$ $CD4^+$ T cells in $Treg^{Ebi3WT}$ surface-Ebi3-positive $CD4^+$ T cells (open circle) versus $Treg^{Ebi3KO}$ animals (closed circle).

(D) Diagram (top left) shows that LNCs from CBA-tolerized $Thy1.2^+$ B6 mice were plated in the upper well of a transwell dish and stimulated with B6, DBA, or CBA antigen. Naive WT-$Thy1.1^+$ B6 mouse or $Ebi3^{KO}$ LNCs were plated in the lower well. Representative flow plots of sEbi3 expression on $Thy1.1^+$ WT (top) or $Ebi3^{KO}$ (bottom) $CD4^+$ T cells in the bottom well after the top well cells were stimulated overnight with media, CBA, DBA, and/or B6 antigen are shown (bottom left). The frequency of $sEBi3^+$ $Thy1.1^+$ CD4 T cells in the bottom well (bottom middle) or $Ebi3^{KO}$ $CD4^+$ T cells (bottom right) was plotted, with a representative image above. The percentage positive for each mouse was determined above media (unstimulated) background (bottom right). Data are from 2–4 experiments of 3–14 mice/group. Significant differences between groups were determined by Man-Whitney *U* tests and ANOVA.

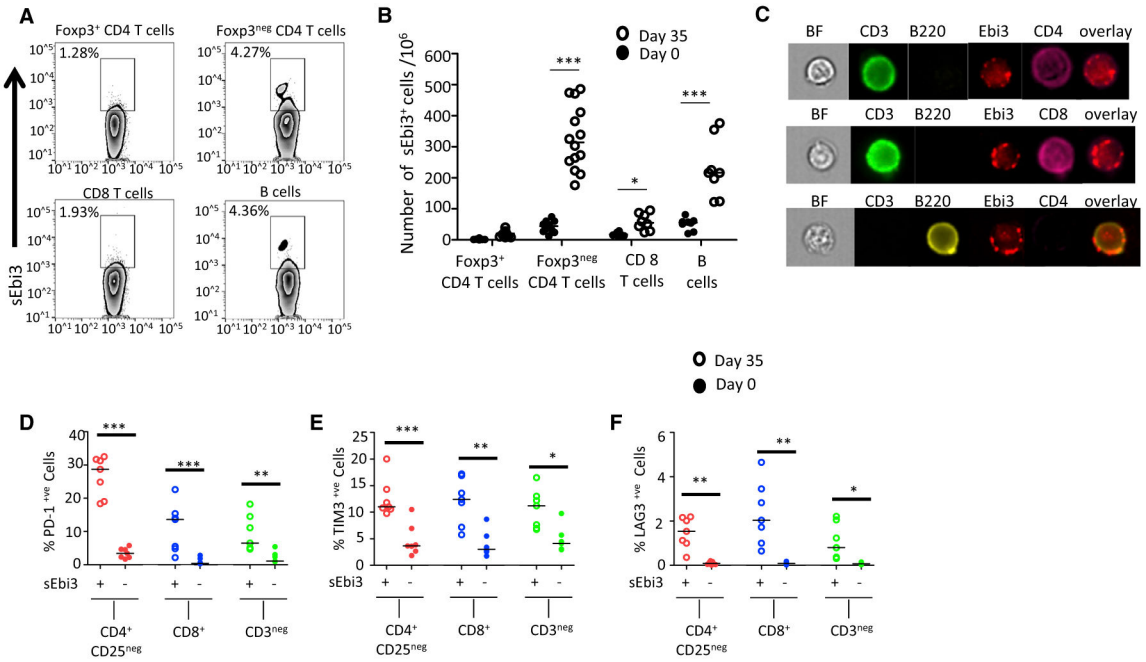

Figure 2. Effects of sEbi3^{+} EV Acquisition (Exogenous Expression) upon *Ex Vivo* Expression of Inhibitory Receptors in CD4^{+} and CD8^{+} T Cells, as well as Non-T Lymphocytes

T and B lymphocytes were harvested from Treg^{Ebi3wt} mice on day 0 and day 35 in independent experiments. To focus on exogenous expression, cells with sEbi3^{+} phenotype in the presence of internal Td^{Tom} signal (producers) were excluded from analysis.

(A) Representative standard flow cytometry examples of Foxp3^{+} CD4^{+} T cells, Foxp3^{neg} CD4^{+} T cells, CD8^{+} T cells, and B cells positive (B220^{+}) for sEbi3 on day 35 post-tolerization.

(B) Quantified flow cytometry data of LNCs from the indicated lymphocyte populations indicating the total number of sEbi3-positive cells before and after 35 days of CBA tolerization using DST and anti CD154. y axis is the number of sEbi3^{+}/10^{6} LNCs (n = 7–14 mice/group). Data were analyzed by Mann-Whitney *U* test (**p < 0.01; ***p < 0.001).

(C) Representative imaging flow cytometry examples of sEbi3^{+} CD4^{+} T (top), CD8^{+} T (middle), and B cells (bottom).

(D–F) Plotted frequency of PD1^{+} (D), TIM3^{+} (E), or LAG3^{+} (F) cells in populations of either sEbi3^{+} cells or sEbi3^{neg} cells among CD4Tconv (CD4^{+}/CD25^{neg}), CD8T, and non-T lymphocytes are shown on day 35 post-tolerization. Data are from n = 7 mice/group.

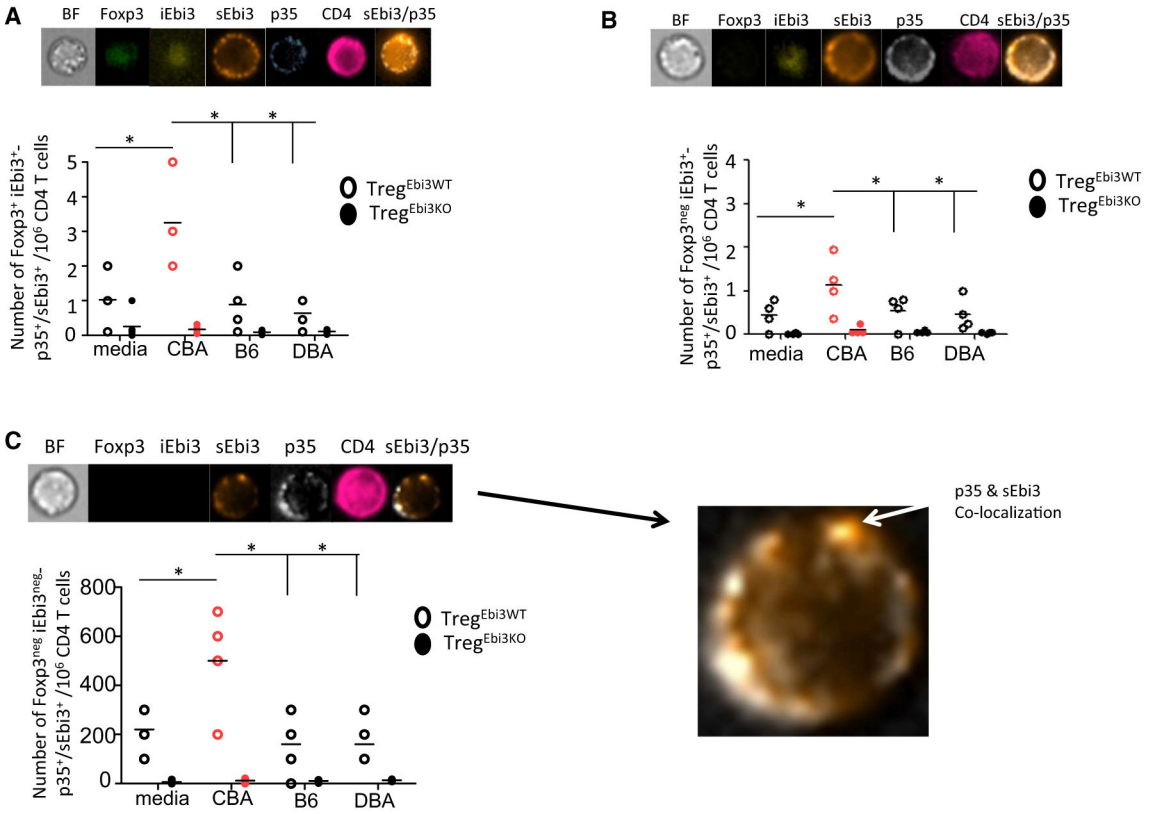

Figure 3. Detection of Surface-Bound Ebi3 and p35 by Allo-Specific CD4$^+$ T Cells

(A) Top: representative imaging flow cytometry example showing the staining pattern for sEbi3 and p35 on a Treg cell that produces Ebi3 following CBA + anti-CD154 tolerization. Bottom: graph indicating the total number of Treg^{Ebi3WT} CD4$^+$ T cells that express both surface Ebi3 and p35 (open circle) were significantly increased at day 35 day post-tolerization following restimulation with control media, CBA, DBA, or B6 antigen. Treg^{Ebi3KO} mouse controls remained negative after all restimulations (closed circle).

(B) Top: representative imaging flow cytometry example showing the staining pattern for sEbi3 and p35 on an iTr35 T cell following CBA + anti-CD154 tolerization (bottom). Graph indicating the total number of such T cells that express both surface Ebi3 and p35 (open circle) were significantly increased by CBA, but not media control, B6, or DBA antigen restimulation, at day 35 post-tolerization versus Treg^{Ebi3KO} controls (closed circle).

(C) Top: representative imaging flow cytometry staining of sEbi3 and p35 on a conventional non-Treg, Ebi3 non-producing, CD4$^+$ T cell 35 days after tolerization (bottom). Overnight CBA stimulation of LNCs from day-35-tolerized mice shows an antigen-specific increase in the number of sEbi3$^+$ and p35$^+$ Foxp3-negative iEbi3-negative CD4$^+$ T cells in Treg^{Ebi3WT} (open circle) versus Treg^{Ebi3KO} mice (closed circle). View to the right indicates those places on the cell surface where sEbi3 and p35 are co-localized and where IL-35 would reside. Data are from 4–7 mice/treatment group. *p ≤ 0.05. Significant differences between groups were determined by Mann-Whitney *U* tests and ANOVA.

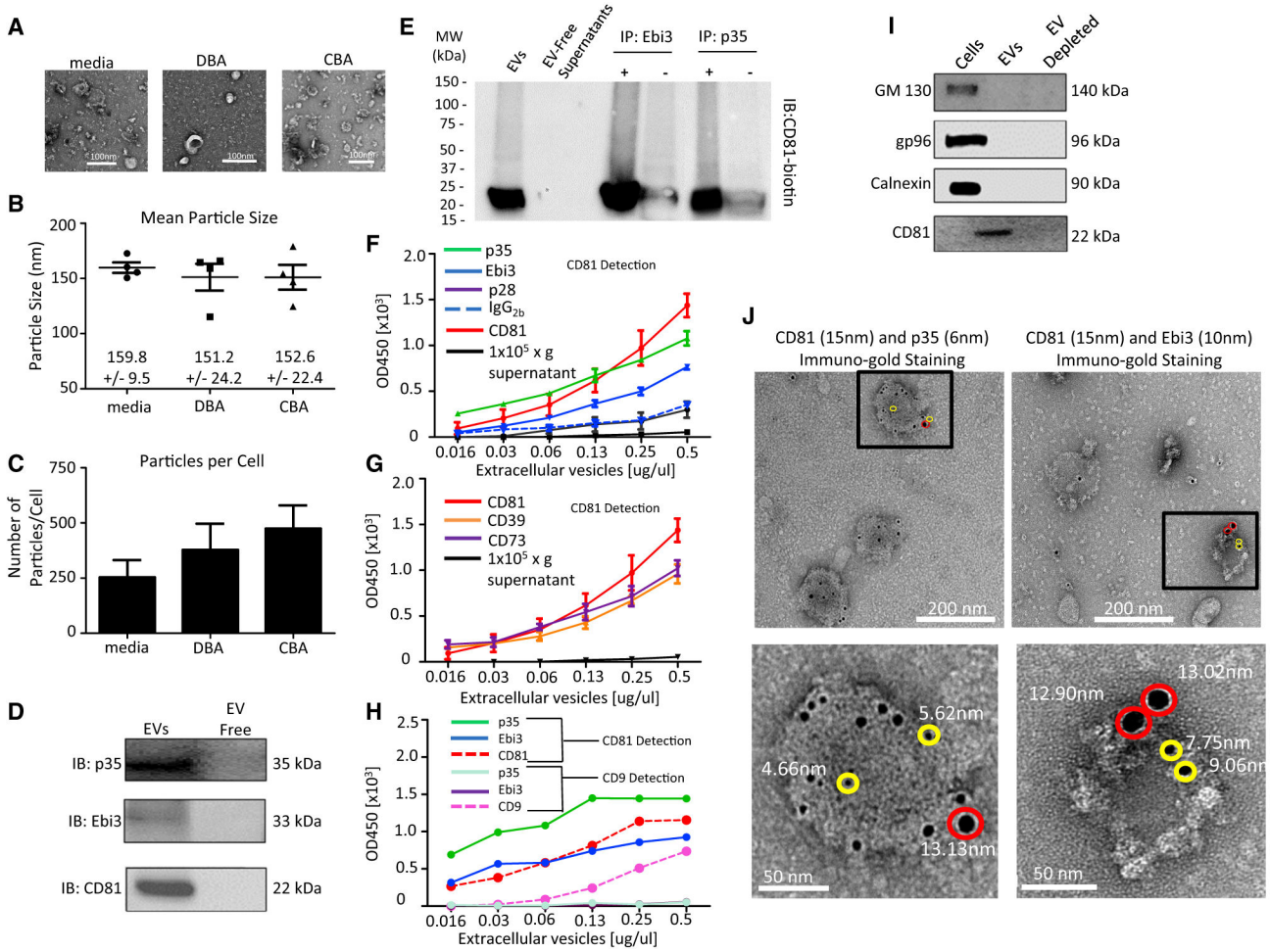

Figure 4. IL-35 Activity Lies within CD81$^+$ EV Fraction of Culture Supernatant

Electron microscopy analysis of EV-fraction, day 35 culture supernatant of antigen restimulated B6 lymphocytes.

(A) Representative negative stain images (100 nm) of EVs collected after media, DBA, and CBA restimulation.

(B)Mean particle size (MPS) of EVs prepared from supernatants of control, DBA, or CBA restimulated cultures of day 35 CBA-tolerized C57/BL6 WT mice.

(C) NTA-determined particle concentration of EVs corrected for number of live cells in culture after overnight restimulation of indicated antigens.

(D) EVs isolated from CBA-tolerized B6 mice were collected from culture supernatant of CBA-tolerized mice restimulated overnight with CBA antigen and analyzed by western blot. Both IL-35 subunits and CD81 were detected in the EV fraction, but not the EV-free fraction.

(E) Immunoprecipitation experiments confirm that isolated EVs contain Ebi3 and p35 protein that co-precipitates with CD81 under non-reducing conditions.

(F) CD81 ELISA analysis of the EV fraction (100,000 × *g* pellet) of day 35 spleen cell/donor antigen co-culture supernatants and the EV-free fraction shows capture of CD81$^+$ EVs with antibodies to CD81, along with antibodies to subunits of IL-35 (p35 and sEbi3, top).

The p28 capture (IL-27) signal was the same as IgG_{2b} background. No signal was detected in the 100,000 × *g* supernatant over the entire dilution range.
(G) CD81 ELISA analysis of CD39 and CD73 capture shows a pattern similar to p35 and Ebi3 throughout the dilution range.
(H) To confirm the specificity of the EVs collected from cultures of antigen-specific cells, ELISA experiments were also performed with CD9 antibodies for detection. Neither IL-35 subunit (p35 or Ebi3) was detected with CD9 antibodies, whereas both IL-35 subunits were detected in CD81 EVs across the entire concentration range. $CD9^+$ EVs were present, as combined anti-CD9 capture and detection gave a low but positive ELISA signal.
(I) Western blot of Golgi (GM130), ER (gp96, Calnexin), and tetraspanin (CD81) in B6 spleen cell fractions, showing enrichment of CD81 in the EV (100,000 × *g* pellet) fraction of the cell supernatant.
(J) Representative TEM images after immuno-gold double antibody labeling, with CD81 and p35 (left) or CD81 and Ebi3 (right) of purified EVs isolated from culture supernatants of CBA-tolerized C57/BL6 mice. High-resolution images show individual EVs with CD81 and p35 or CD81 and Ebi3 co-staining. Data are from 4–5 mice/treatment group. Error bars represent SEM of analyzed data. **$p \leq 0.01$. Significant differences between groups were determined by Mann-Whitney *U* tests and ANOVA.

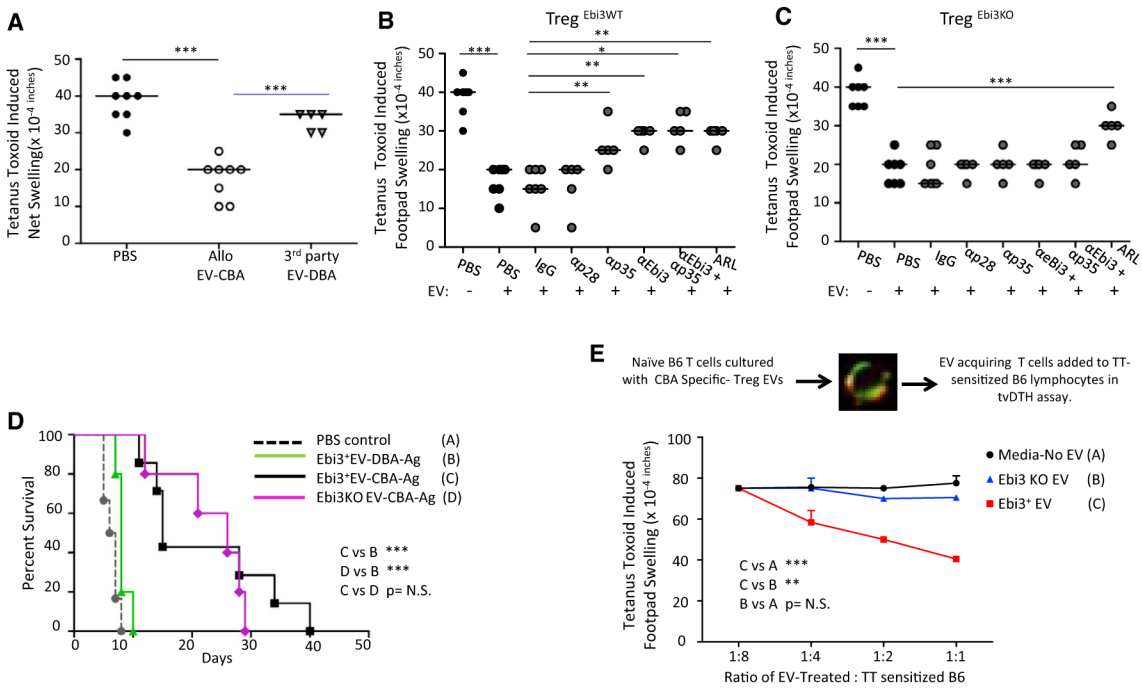

Figure 5. Donor-Specific Linked Suppression and Graft Prolongation by EVs from Allo-Specific Treg Cells: Requirement of IL-35 for Secondary Suppression

(A–C) Isolated EVs from culture supernatants of CBA-tolerized B6 lymphocytes reproduce IL-35-dependent tvDTH-linked suppression. Lymphocytes harvested from TT/DT-immunized WT B6 mice were used as responder cells in tvDTH.

(A) Antigen specificity of EV production in tvDTH linked-suppression response. The tvDTH-linked suppression of recall response was caused by CBA, but not DBA, restimulated culture EVs (n = 5–8 $Treg^{Ebi3WT}$ mice/group).

(B and C) tvDTH assays were performed by co-injecting lymphocytes with the indicated neutralization antibodies in footpads with TT/DT alone or along with the EV. Two types of ultracentrifuge-purified EV from CBA restimulated spleen cells of tolerized $Treg^{Ebi3WT}$ mice (B) and tolerized $Treg^{Ebi3KO}$ mice (C) were tested; each dot represents EVs from lymphocyte culture supernatant of an individual mouse (n = 5–7 mice/group) analyzed by Mann-Whitney *U* test (**p < 0.01; ***p < 0.001).

(D) CBA recipient mice were transplanted with a B6 heart allograft and treated intraperitoneally with PBS (control) or EVs from allo-specific CBA or third-party DBA/2 co-cultures with tolerized B6 responder cells. Graft survival estimation and differences in the survival rates were analyzed by the Kaplan-Meier method and log-rank test, respectively (n = 5–6 mice/group).

(E) Top: panel depicts a naive B6 T cell expressing surface Ebi3 (red) and p35 (green) after overnight co-culture with EV from $EBi3^{WT}$, CBA-tolerized B6 hosts prior to addition to the TT-responsive B6 splenocytes in tvDTH assays. EV-acquiring naive B6 T cells develop the ability to cause secondary suppression of anti-TT responder T cells in tvDTH assays (red line) throughout various ratios of EV-treated to TT-sensitized B6 cells. This ability was lost when the EVs used to treat the B6 lymphocytes were derived from CBA-tolerized mice in which the production of Ebi3 (hence IL-35) has been selectively deleted in $Foxp3^{+}$ T cells

(blue line). Error bars represent SEM of data analyzed by Mann-Whitney *U* test (**p < 0.01; ***p < 0.001).

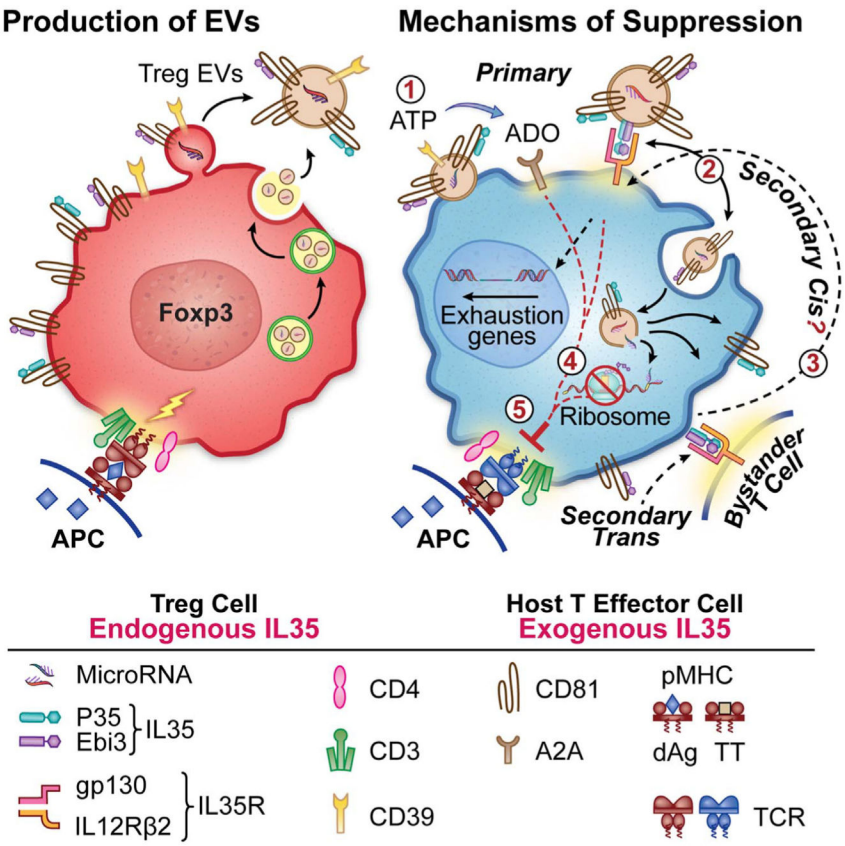

Figure 6. Model of Treg-Cell-Derived sEbi3^{+} EV-Mediated Tolerance in Transplantation

Tissue-resident Treg cells (donor, red, left) produce IL-35-coated EVs in response to familial antigens upon living related graft placement via either a multivesicular body-plasma membrane fusion or direct budding of EVs from the plasma membrane. The EVs also contain CD39 (1) and CD73 (not shown) converting extracellular ATP to adenosine (ADO; step 1), as well as miRNA "cargo," also contributing to primary suppression (step 4). Components of IL-35, Ebi3 and p35, are shown "bracketing" the tetraspanin CD81 (steps 2 and 3) on both the producing, graft-resident Foxp3 Treg cell surface and the IL-35-acquiring, host T effector cell (recipient, blue, right). The IL-35 components reassemble at nodes that bind the high-affinity IL-35R (gp130/IL12Rβ2), altering the microenvironment of the graft such that bystander T cells (far right) entering the graft undergo secondary *trans* suppression, while the modified effector itself undergoes secondary *cis* suppression by repeated engagement of its own IL-35R and is eventually exhausted, leading to expression of inhibitory receptors.

KEY RESOURCES TABLE

REAGENT or RESOURCE	SOURCE	IDENTIFIER
Antibodies		
Anti - CD81	Cell Signaling Tech	D502Q
Anti-p35	R and D Systems	#MAB6688
Anti- Ebi3	Shenandoah Biotech or a gift from the lab of D. Vignali	V1.4H6.29
Anti CD127-Biotin	Miltenyi Biotec	130-101-910
Anti-CD19-Biotin	Miltenyi Biotec	130-101-951
Anti- LAG3-APC	Biolegend	C9B7W
Anti-TIM3-PE	eBioscience	8B.2C12
Anti-Foxp3-e660	Invitrogen	FJK-16 s
Anti-CD127-PECF594	BD Biosciences	SB/199
Anti-CD81-PE	Biolegend	#104905
Anti-CD25 PECy7	BD Biosciences	PC81
Anti-B220 APC/Cy7	Biolegend	103224
Anti-CD19 FITC	BD Biosciences	553785
Anti CD3 BUV737	BD Biosciences	145-2C11
Anti CD4 BUV395	BD Biosciences	GK1.5
Strepavidin – PECF594	BD Biosciences	562318
Anti CD25 BV421	BD Biosciences	M-A251
Anti CD8 PE	BD Biosciences	53-6.7
Anti CD8 BV605	Biolegend	53-6.7
Strepavidin - APC	BD Biosciences	554067
Anti PD-1 PECy7	Biolegend	109109
Anti LAG3 BV785	Biolegend	C9B7W
2W1S Tetramer -APC	NIH Tetramer Core	N/A
2W1S Tetramer - PE	NIH Tetramer Core	N/A
Anti-TGFβ	BD Biosciences	A75-2
Anti-IL10	R and D Systems	JES052A5
Anti-IL4	BD Biosciences	11B11
Anti-CD81-biotin	Thermo Scientific	MA5-17938
Anti-CD81	Cell Signaling	D5O2Q
Anti-CD9-biotin	Biolegend	MZ3
Anti-CD9	eBioscience	eBioKMC8
Anti-CD9	Abcam	EPR2949
Biological Samples		
CBA spleens for sonication/tolerization	Jackson Laboratory	https://www.jax.org/strain/000654
2W1S mouse spleens for sonication/tolerization	Courtesy of Drs. Marisa Alegre and Anita Chong; University of Chicago	https://immunology.uchicago.edu/program/faculty/maria-luisa-alegre
Chemicals, Peptides, and Recombinant Proteins		
Anti CD40L	BioXcell	MR-1; BE0017-1
ECL Western Blotting Substrate	Thermo Fisher	#32106

REAGENT or RESOURCE	SOURCE	IDENTIFIER
Glutaraldehyde 10%	Electron Microscopy Sciences	#16100
Protein G Sepharose 4 Fast Flow	GE Healthcare	17-0618-02
Critical Commercial Assays		
IL-10 mouse ELISA	R and D Systems	SM1000B
Regulatory T cell Isolation Kit	Miltenyi Biotec	130-091-041
Experimental Models: Organisms/Strains		
Foxp3$^{Cre\text{-}YFP}$ mice	Jackson Laboratory	#016959
Ebi3^{Tom} mice	Dario Vignali (University of Pittsburgh, PA)	N/A
Ebi3$^{TomL/LThy1.1}$ mice	Dario Vignali (University of Pittsburgh, PA)	N/A
C57BL/6 mice	Jackson Laboratory	#000664
Software and Algorithms		
GraphPad Prizm	GraphPad Software	https://www.graphpad.com/support/
Flowjo	Becton Dickinson	https://www.flowjo.com/about/company
IDEAS Software	Amnis –Luminex Corporation	https://www.luminexcorp.com/imagestreamx-mk-ii/
ImageJ	public domain	https://imagej.nih.gov/ij/
Other		
1.0uM Trans-well insert	Corning: Millipore Sigma	https://www.sigmaaldrich.com/catalog/product/sigma/cls3392?lang=en&region=US
300-Mesh Carbon/formvar-Nickel grids	Electron Microscopy Sciences	https://www.emsdiasum.com/microscopy/products/grids/support.aspx
Aurion Immuno-gold Beads 15nM-Strepavidin	Electron Microscopy Sciences	#25272
Aurion Immuno-gold Beads 10nM – Goat α Mouse IgG	Electron Microscopy Sciences	#25128
Aurion Immuno-gold Beads 6nM – Goat α Rat IgG	Electron Microscopy Sciences	#25188
12% Tris-HCL Ready Gel	Bio-Rad	#1611114
Exosome Depleted Fetal Bovine Serum	GIBCO- Life Technologies	A27208-03
Diptheria and Tetanus Toxoid Pediatric Vaccine	Sanofi Pasteur	NDC 49281-225-10